A Review on the Solar Air Heater Thermal Performance Enhancement Techniques: Artificial Roughness

[1]Yogeshkumar D. Khimsuriya, [2]Hiren T. Patel, [3]Amitkumar J. Shaparia

[1]Research Scholar, Mechanical Department, Mahatma Gandhi Institute of Technical Education & Research Centre, NPE Campus, Bhanunagar, Eru – Aat Road, Jalalpore, Navsari, Gujarat, India
[2]Faculty of Engineering, Mahatma Gandhi Institute of Technical Education & Research Centre, NPE Campus, Bhanunagar, Eru – Aat Road, Jalalpore, Navsari, Gujarat, India
[3]Assistant Professor, Prime Institute of Engineering and Technology, Navsari, Gujarat, India

***Abstract*: Solar air heater is very simple, basic, eco-friendly and economical device for harnessing the solar energy and it has been widely used across the world for many domestic and industrial applications. The lower thermal efficiency of the SAH has directed the focus of the researchers to improve the thermal efficiency of the SAH. There is generation of the laminar viscous sub layer near the absorber plate which reduces the thermal performance of the SAH. Breaking this laminar sub layer and creating the turbulence in the fluid flow field will help to improve the heat transfer. This paper discusses the various methods, designs and roughness geometries used by various researchers to improve the performance of the SAH. Designs, roughness geometries and their impact on the heat transfer, Nusselt number (Nu) and Friction factor (fr) have been summarily discussed.**

***Keywords*: Solar air heater, Roughness Geometries, Reynolds's number, Nusselt number, Friction factor**

1. Introduction

Energy is the basic need of life all over the world and it also affect the life standards of the human society in a variety of way. Rapid industrialization causes huge demand of energy all time for sustainable development [1]. The consumption of energy is directly proportional to the progress of mankind. With ever growing population, improvement in living standard of the humanity, industrialization of developing countries, the global demand of energy is expected to increase rather significantly in the near future. India rank fifth in the world in total energy consumption and needs to accelerate the development of the sector to meet its growth aspiration. India has one of the fastest and largest growing economies in the world, as well as an expensive populace of above 1.17 billion people. There is a very high demand for energy, which is currently satisfied mainly by coal, foreign oil, and petroleum, which apart from being a non – renewable, and therefore non – permanent solution to the energy crisis; it is also detrimental to the environment. Thus, it is essential to tackle the energy crisis through judicious utilization of abundant the renewable energy resources, such as biomass energy, solar energy, wind energy, geothermal energy and Ocean energy [2] .

Non-conventional energy sources are truly a gift from the Gods. Wind & solar energy perhaps their most bountiful. India today has among the world's largest programmes in solar energy. A sizeable research and technology base, a grooving manufacturing capability, and a country-wide infrastructure for the distribution and after sale service of solar energy products have emerged. Solar energy is beginning to be used for a large number of applications. Nevertheless, the achievements so far add up only to a tiny fraction of what is needed and what is possible [3].

Solar energy is the most widely used renewable source of energy because it is easily available, can be easily converted and stored in other form of energy. There are mainly two types of solar energy: (1) Active solar energy and (2) Passive solar energy. In Active solar energy, the solar energy is converted and stored in other form of energy using equipment, whereas in Passive solar energy, no equipment is used to convert the solar energy and the energy is directly used where needed. The Sun radiates energy at the rate of $3.7 * 10^{22}$ MW from which about $1.85 * 10^{22}$MW of energy reaches the earth atmosphere. This sun's energy is collected through systems and then it is converted into heat or electricity. This converted solar energy can be used for cooling/heating purpose to reduce the size and cost of the equipment and obtain more efficiency of the machinery [4].

Solar thermal collectors are the technologies widely used for converting the solar energy into the thermal energy. Solar radiation incident on the surface of the collector are absorbed by the absorber and then converted into the heat energy and stored. The stored heat energy is transferred to the working fluid. Solar collectors are mainly used for the heating water but they also used in different applications. There are several types of the solar collectors available in the market which has been used for different applications. There are also some collectors used in building infrastructures are called as building-integrated solar thermal systems. Solar thermal collectors are generally classified as concentrating, non-concentrating and hybrid systems also called as photovoltaic collectors Fig. 1. [5]

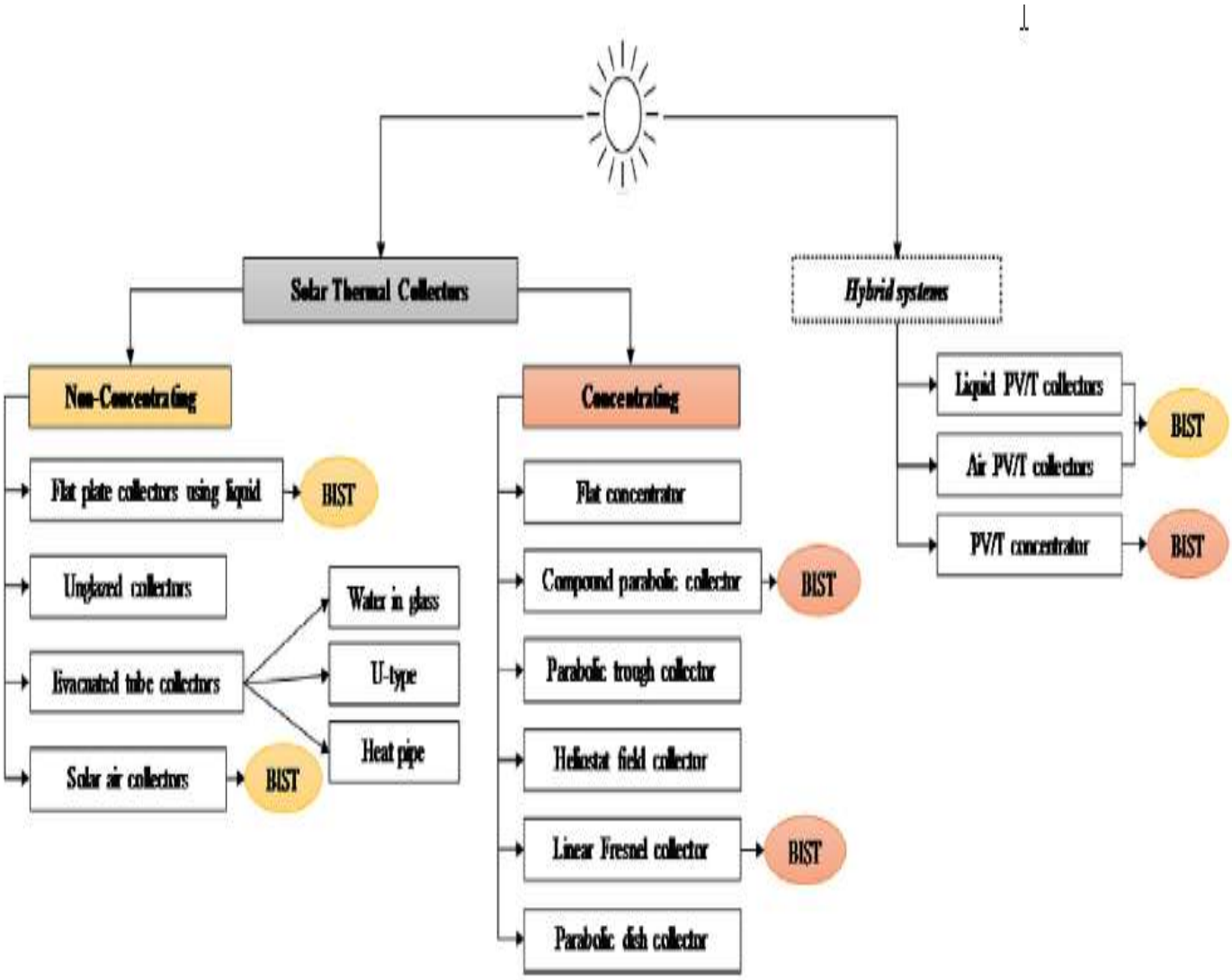

Figure 1 Solar system classifications [5]

Solar air heater is one of the non-concentric type solar thermal collectors. It collects the solar radiations and stores them in a absorber plate and converts into the heat energy. It is very easy in construction and low cost system. It is widely used in low to moderate level domestic and industrial thermal applications. The basic construction of SAH is shown in Fig. 2 [6]. It consists of absorber tray, glass cover as glazing, inlet and outlet openings and insulation. Glazing will help the absorber tray to absorb more solar radiation also reduces the heat loss to the atmosphere. Insulation also reduces the thermal loses of the system. Solar air heaters are classified as shown in Fig. 3 [7].

SAH has wide range of applications crop drying, fruit drying, timber drying, and space heating, solar induced ventilation. In these applications temperature required ranges from 40-80°C [8]. Solar air heater is also used for moulding sand dryers in foundries, laundry applications, sterile environment, HVAC systems, solar refrigeration and air conditioning, SAH assisted humidification and dehumidification desalination systems [9-11].

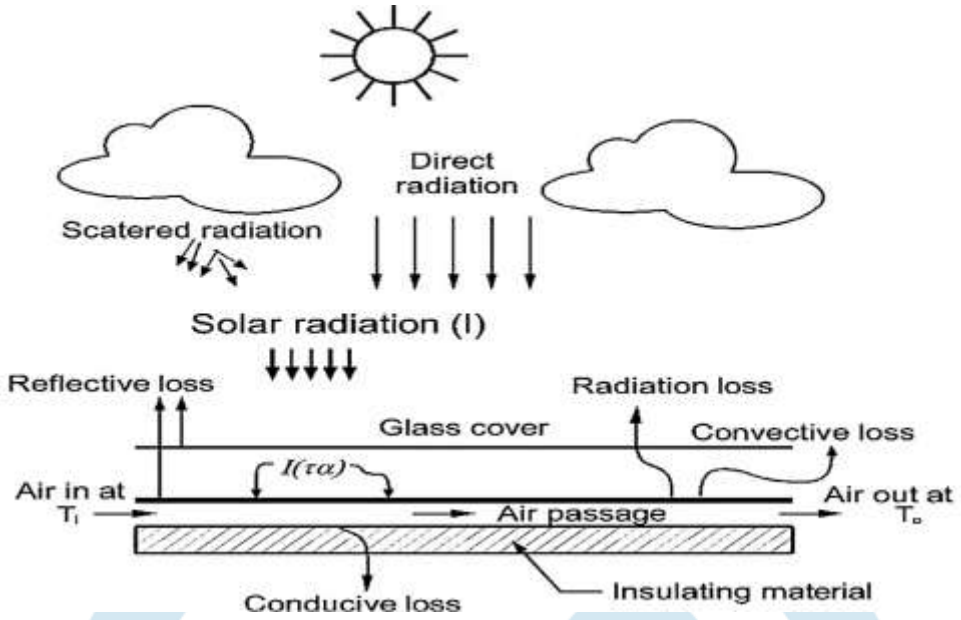

Figure 2 Conventional Solar Air Heater [6]

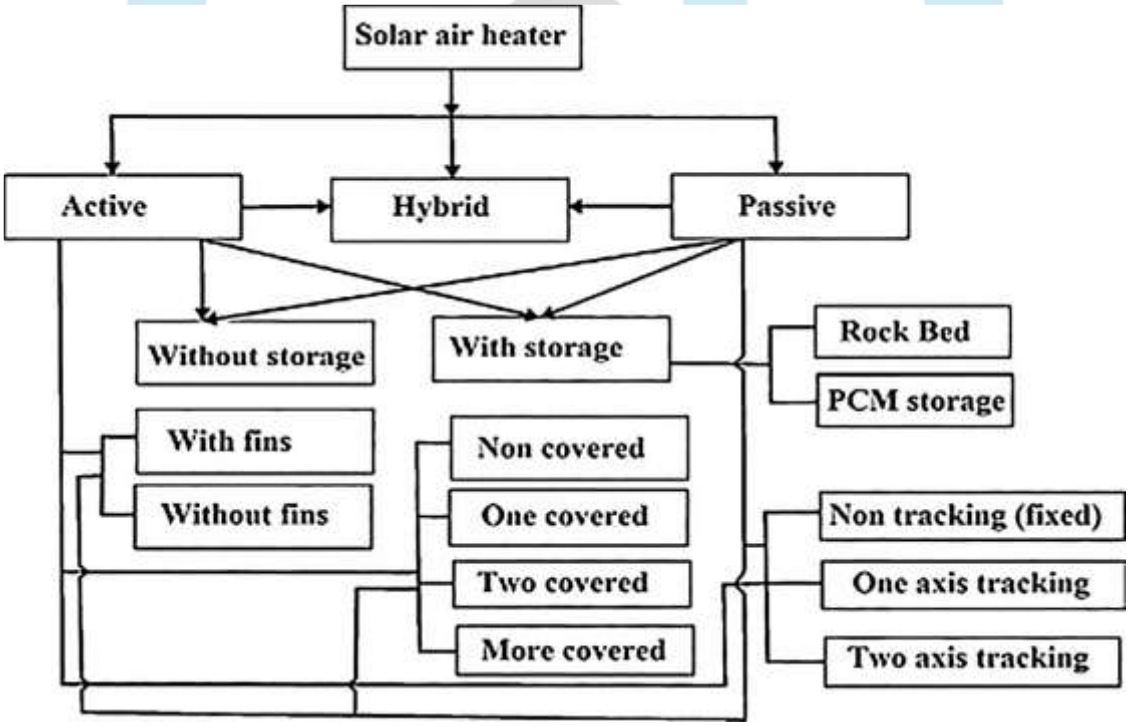

Figure 3 Classification of solar air heating technologies [7]

In a solar air heater when air passing over the absorber plate there is generation of boundary layer. That reduces the heat transfer of the system. Generation of the laminar sub layer near the absorber plate surface opposes convective heat transfer and thus reduces heat transfer co-efficient [12]. Higher the thickness of the laminar sub layer lowers the heat transfer. So it is essential to break laminar sub layer and this can be done by creating turbulence in the fluid flow. There are some methods suggested by researchers to break the laminar sub layer and improve augmentation in heat transfer includes: (i) increasing the roughness of the absorber plate, (ii) employing air impinging jets, (iii) replacing single duct collector by double or multi pass collectors and (iv) introducing baffles [13]. Great efforts have been done for artificially breaking the laminar sub layer causes the thermal resistance because it has considerable impact than any other method [14]. The consecutive artificial roughness geometries used by various researchers to improve the thermal performance of the solar air heater have been discussed in following article.

2. Various roughness geometries used in SAH

2.1 V shape roughness geometries

Dongxu Jin et. al.,[15] numerically investigated heat transfer and fluid flow characteristic in a SAH duct having multi V-shaped ribs on the absorber plate. Three-dimensional simulations was conducted and computation were performed for different rib geometries with varying span wise V-rib number, relative rib pitch, relative rib height and angle of attack for different Reynolds number. They noticed multi V-shaped ribs generate stream wise helical vortex flow which promote the fluid mixing between the colder mainstream fluid and warmer fluid near the absorber wall. The average Nu, friction factor and thermo hydraulic performance parameter all tend to decrease with the increase in relative rib pitch for the range of parameters investigated. An angle of attack 45° gives maximum values of Nu number and the average Nu number and friction factor increases with increasing the relative rib height. Piyush Kumar Jain et. al.,[16] have studied the new V-rib roughness geometry having some fixed parameters as shown in table no.1 and four different rib roughened plates of relative roughness pitch (P/e) of 10, 12, 14, and 16 as shown in fig.4. They have observed that In comparison to the smooth duct V-rib with symmetrical gap and staggered rib gives enhancement of Nusselt number as 2.30 and friction factor as 3.13 whereas for V-rib with symmetrical gap the enhancement in Nusselt number and friction factor is 2.03 and 3.03 times that of smooth plate respectively and for multi gap V-down rib combined with staggered rib the enhancement in Nusselt number and friction factor is 2.27 and 3.35 times that of smooth plate respectively. Relative roughness pitch has major impact on Nu and friction factor and relative roughness of 12 gives maximum Nu and friction factor. Pitak et. al.,[17] investigated that the B-VRs induced longitudinal vortex flows toward the channels, resulting in considerable heat transfer enhancement which accompanied by friction loss penalty.

Table 1. Range of parameters

Parameters	Range of values
Relative roughness height (e/D_h)	0.045
Relative staggered rib pitch (P'/P)	0.65
Relative roughness pitch (P/e)	10, 12, 14, 16
Number of gaps on each side of V rib (N_g)	3
Relative gap width (g/e)	4
Relative staggering rib size (w/e)	4
Duct width (W)	200 mm
Aspect ratio (W/H)	8
Angle of attack (α)	60°

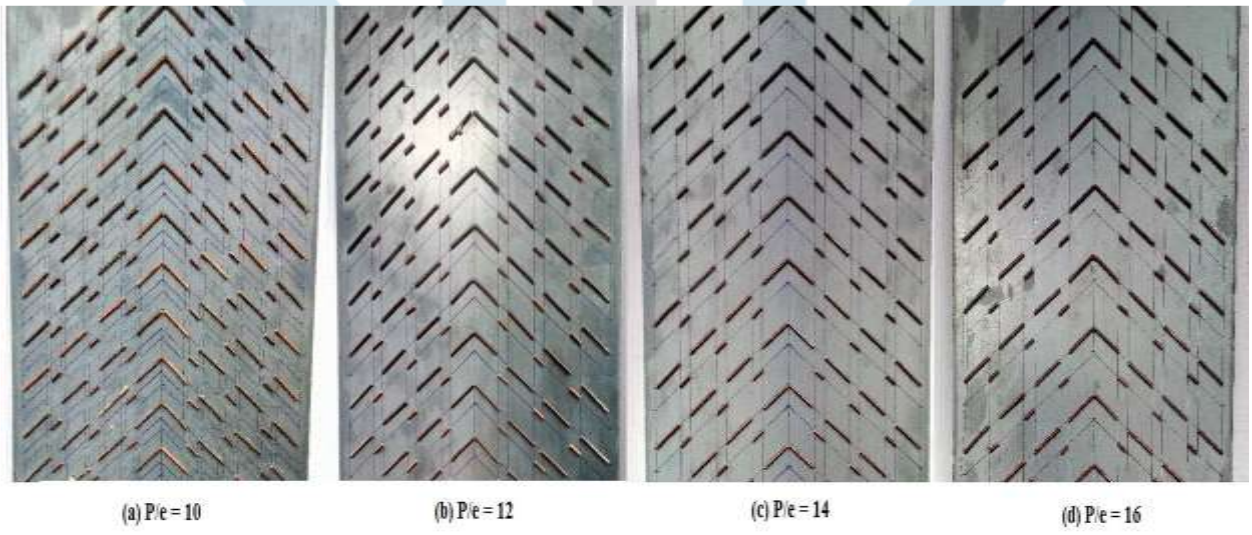

Figure 4 Photograph of absorber plate roughened with V-rib with symmetrical gap and staggered rib of four different relative roughness pitches

V. S. Hans et. al.,[18] carried out experimental study of multiple V-rib roughness on heat transfer co-efficient and friction factor in SAH duct. They have developed the co-relation for Nu number and friction factor. The maximum enhancement of Nusselt number and friction factor has been found to be 6 and 5 times respectively in comparison to the smooth duct. Pongjet promvonge[19] studied heat transfer and pressure drop in a channel with multiple 60° V-baffles. They have kept aspect ratio, height and transverse pitch of the v-baffle as 10, 3 and 2H respectively. And used three different baffle blockage ratio (e/H) as 0.10, 0.20 and 0.30 while pitch spacing ratio varying as 1, 2 and 3. The experimental results show that V-baffle provides the drastic increase in Nusselt number, friction factor and thermal enhancement factor values over the smooth wall channel due to better flow mixing from the formation of secondary flows induced by vortex flows generated by the V-baffle. The use of the V-baffles with e/H=0.30 cause a very high

heat transfer and pressure drop increase as compared with other flow blockage ratios. Sukhmeet Singh et. al.,[20] studied thermo-hydraulic performance of SAH using five different relative roughness pitch 4, 6, 8, 10 and 12 of V-down rib with gap. The Nusselt number and friction factor were found to be highest for relative roughness pitch of 8. Momin et. al.,[21] observed that the rate of increase of Nusselt number with an increase in Reynolds number is lower than the rate of increase of friction factor; this appears due to the fact that at relatively higher values of relative roughness height, the re-attachment of free shear layer might not occur and the rate of heat transfer enhancement will not be proportional to that of friction factor. Deo et. al.,[22] found for the multi gap V-down ribs combined with staggered ribs that Nusselt number increased with increase in the angle of attack and become maximum for the angle of 60°. Its value remained almost same for the angle of 70°, but further increase in the value to 80° lowered the Nusselt number. On the other hand friction factor continued to increase with increase in the angle of attack.

2.2 Roughness geometries with perforation

Tabish Alam et. al.,[23] experimentally investigated heat transfer enhancement for V-shaped perforated blocks as shown in fig.5. They were used range of parameters as shown in table 2. The open area ratio is defined as ratio of the area of the perforation to the block frontal area. Average enhancement in Nusselt number for perforated V-shaped blockages is found to be 33% higher over solid blockage while friction factor of perforated blockages gets decreased by 32% of the values as found in solid blockages.

Table 2. Range of parameters

S. No.	Parameters	Range
1	Reynolds number (Re)	2000-20000(Ten values)
2	Relative blockage height (e/H)	0.4-1(Four values)
3	Relative pitch (P/e)	4-12(Five values)
4	Angel of attack (α)	60° (One value)
5	Open area ratio (β)	5-25%(Five values)

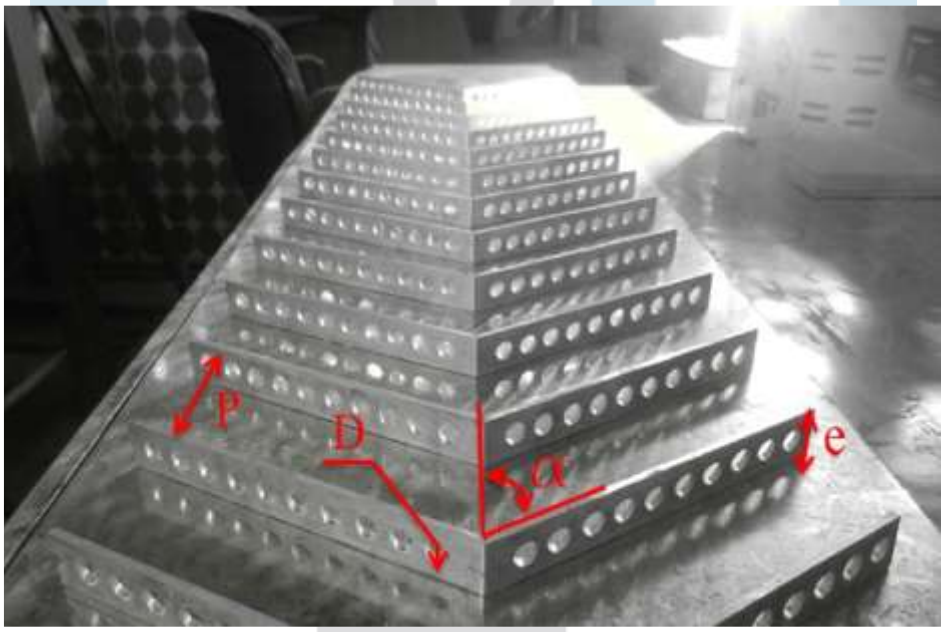

Figure 5 V-shaped perforated blocks

Rajendra Karwa et. al.,[24] extensively investigated heat transfer and friction factor in rectangular duct with half and fully perforated baffles at different pitches. The study shows an enhancement of 79–169% in Nusselt number over the smooth duct for the fully perforated baffles and 133–274% for the half perforated baffles while the friction factor for the fully perforated baffles is 2.98–8.02 times of that for the smooth duct and is 4.42–17.5 times for the half perforated baffles. Tabish Alam et. al.,[25] The effect of circularity of perforation holes, relative pitch ratio, relative blockage height, open area ratio and angle of attack on Nusselt number and friction factor has been studied for flow Reynolds number range of 2000–20,000. Non-circular perforation holes was been found to result in higher heat transfer as compared to circular holes with same open area ratio; and there is optimum non-circular shape that corresponds to a circularity of 0.69. Maximum enhancement in Nusselt number and friction factor is found to correspond to an angle attack value of 60°.Circularity (ψ) is representative of closeness of hole to a circular shape and is defined as the ratio of parameter 'Pe' of equivalent circle having the same cross-section area as that of a non-circular shaped hole to the perimeter 'p' of this non-circular hole fig.6.

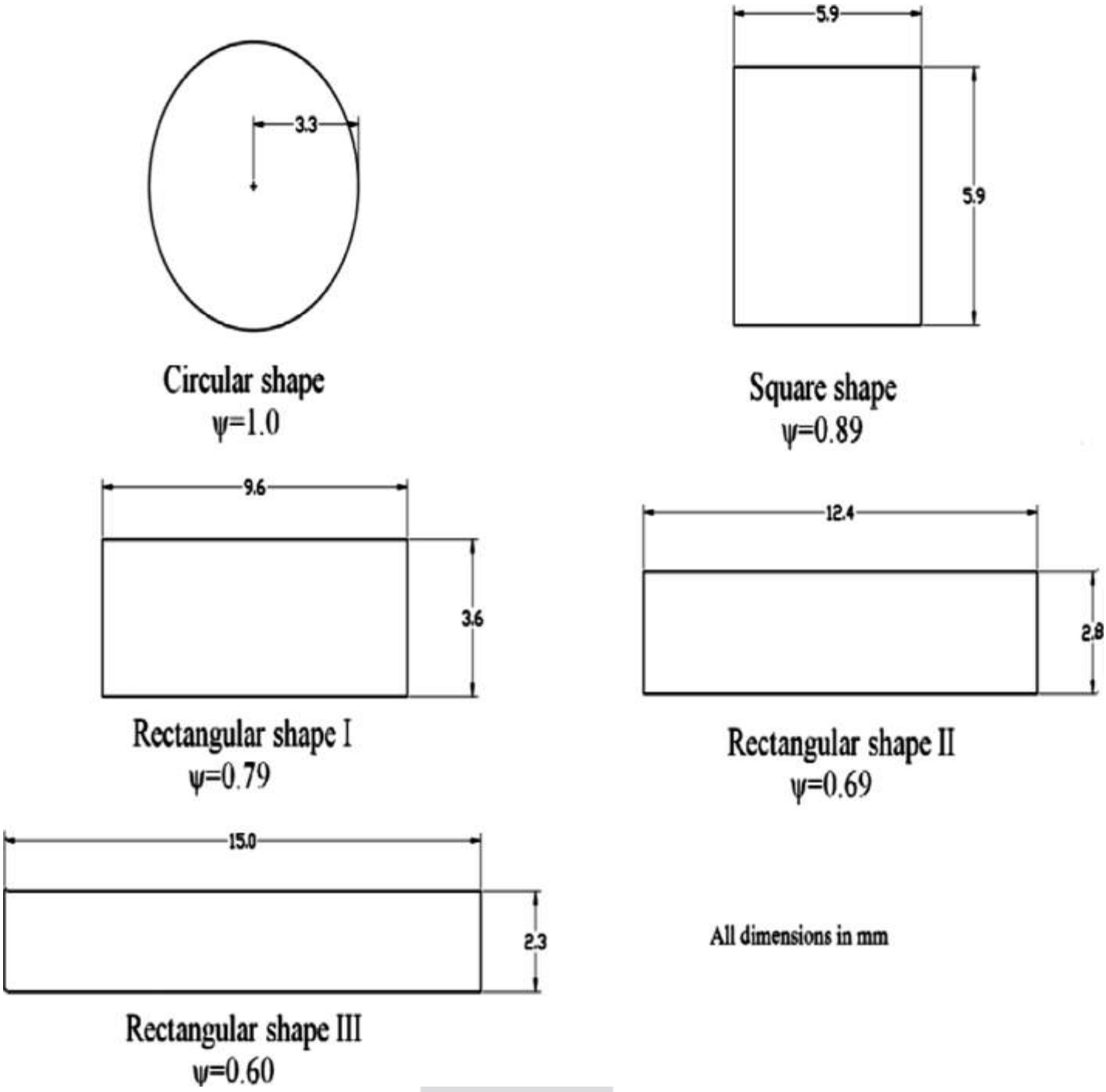

Figure 6 Five different shapes of perforation

Sompol Skullong et. al.,[26] studied experimental and numerical fluid flow and thermal behaviours of perforated winglet type vortex generators. They were studied rectangular and trapezoidal type of winglet vortex generators and investigated the effect of perforation on them. Friction loss decreases in perforated winglet vortex geometry. The 30° P-RWVG with d = 1 yields the highest Nu_R and f_R of about 6.78 and 84.32 times. Hwang et. al.,[27] observed that since a part of the airflow passes through the perforated rib and directly impinges on the recirculating bubble behind the rib, hot-spots occurring in the region around the concave corner behind the solid-type rib do not arise in the corresponding region of the perforated-rib geometry. Sara et. al.,[28] concluded that for the perforated blocks, the higher the perforation diameter, perforated area open area ratio and the inclination of perforation holes, the better the overall energy performance. Liou et. al.,[29] concluded that for the ranges of Reynolds number and H/D_e examined the thermal performance (Nu_p) attained by the studied detached perforated type ribbed duct is as high as 1.3-1.9 times that attained by a smooth duct (Nu_s^*) at the same pumping power.

2.3 Z shaped baffles

Parkpoom Sriromreun et. al.,[30] experimentally and numerically studied for heat transfer enhancement in a channel with z-shaped baffles. They have used three baffles to channel height ratio as 0.1, 0.2, and 0.3 and three baffle pitch ratios as 1.5, 2 and 3. Z baffles

create co-rotating vortex flows will leads to enhancement in heat transfer. The Nusselt number , friction factor and thermal performance enhancement factor for the in-phase 45° Z-baffles are found to be considerably higher than those for the out-phase 45° Z-baffles at a similar operating conditions. The in-phase Z-baffles with e/H=0.1, P/H=1.5 provides the highest TEF at about 2.2 at the lowest Re.

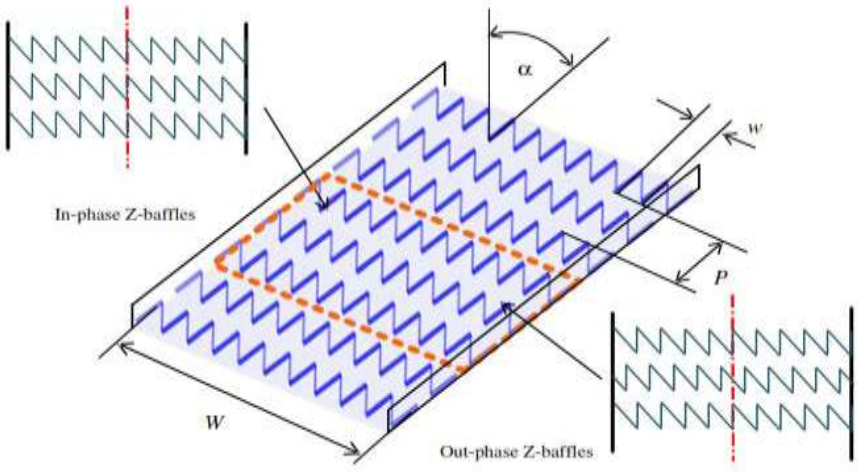

Figure 7 Test section with in-phase and out-phase Z-baffles arrangements

2.4 Dimple shaped roughness

Muneesh Sethi et. al.,[31] carried out an extensive experimental study to predict the heat transfer and flow characteristics of SAH having dimple shaped artificial roughness arranged in an angular fashion as shown in fig.8. Nusselt number increases whereas friction factor decreases with the increase in Reynolds Number. The maximum value of Nusselt number has been found corresponding to relative roughness height of 0.036, relative roughness pitch of 10 and arc angle of 60°.The statistical correlation for Nusselt number and friction factor has been developed as a function of Reynolds number and roughness geometry parameters. In the range of studied parameters, the maximum deviation for Nusselt number and friction factor has been found to be ±8% and ±8% respectively. Vikash kumar[32] investigated SAH with concave dimple roughened ducts on 1 & 3-sides of the absorber plate. The maximum enhancement in Nu for varying p/e, e/D_h & e/d wad respectively found to be of the order of 2.6 to 3.55 times, 1.91 to 3.42 times and 3.09 to 3.94 times than one side concave dimple roughened duct for the parameters range investigated. Same way minimum and maximum rise in f of 3-sides over 1-side roughened duct for varying p/e, e/D_h & e/d was respectively found to be as 1.62 to 2.79 times, 1.52 to 2.34 times and 2.21 to 2.56 times.

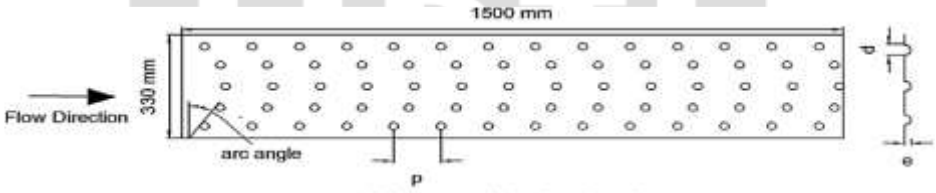

(a) Diagram of the absorber plate

(b) Pictorial view of the absorber plate

Figure 8 (a) Diagram of the absorber plate. (b) Pictorial view of the absorber plate

2.5 Multiple broken transverse ribs roughness

Inderjeet Singh et. al.,[33] investigated two novel ribs arrangements namely multiple broken transverse ribs and square wave shaped ribs (fig.9) for performance enhancement of SAH. The parameters use are as P/e=10, e/D=0.043 and W/w=7 for both arrangements

and investigated at six levels of Reynolds number ranging from 3000 to 8000. Maximum thermal enhancement of 2.50 times with corresponding pumping power penalty of 3.92 times is obtained for square wave shaped ribs whereas in case of multiple broken ribs, the enhancements are 3.24 and 3.85 times respectively.

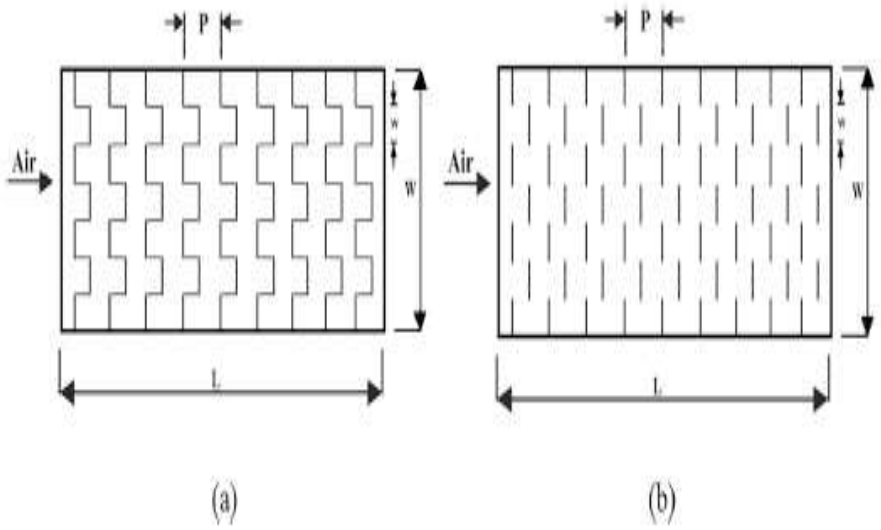

Figure 9 SAH duct roughened with (a) Square wave shaped ribs (b) Multiple broken transverse ribs

Varun et al.,[34] experimentally investigated solar air heater with transverse and inclined ribs as shown in fig.10. The range of parameters have been investigated are Re 2000-14000, relative roughness pitch 3-8, and fixed value of relative roughness height 0.038. They have found maximum effective efficiency at relative roughness pitch of 8.

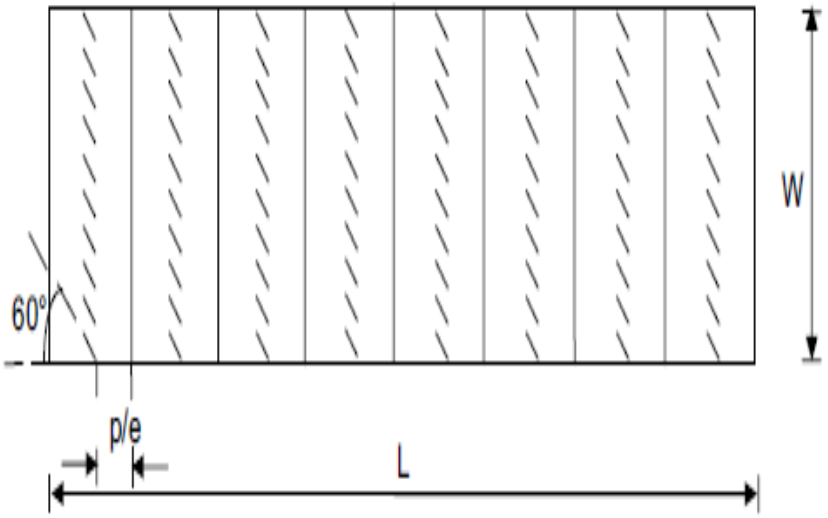

Figure 10 Absorber plate showing the roughness element

2.6 S-Shaped rib roughness

Dengjia Wang et al.,[35] studied S-shaped roughness with gap (fig.11) to evaluate the performance of the SAH. Thermal efficiency of roughened solar air heater is significantly higher compare to smooth solar air heater. The maximum augmentation achieved in *Nu* and f is 5.42 and 5.87, respectively. The maximum enhancement for *Nu* takes place at the Reynolds number *Re* = 19,258, relative rib width W/w = 4, relative rib spacing p/e = 20, and relative gap spacing g/e = 1.5. The maximum thermal efficiency of collector can be increased by about 30% for the air channel height in the range from 30 mm to 50 mm, and the pressure drop is significantly increased.

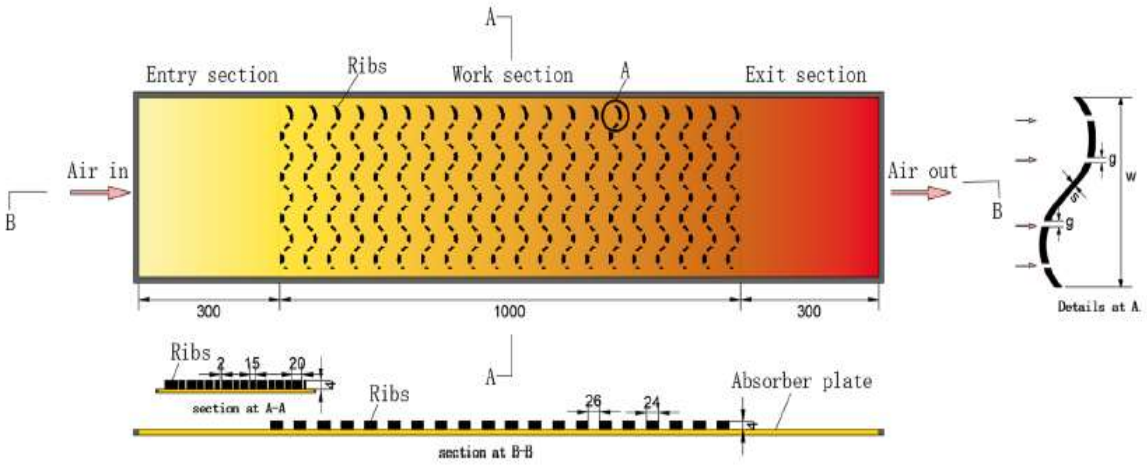

Figure 11 Ribs arrangement on collector plate

2.7 C-shaped artificial roughness

Mohitkumar et al.,[36] experimentally examined multiple C-shape rib to evaluate the thermal and hydraulic performance of double flow SAH as shown in fig.12. They were used three roughness angles and five pitch distances. Maximum Nusselt number was 415 obtained for relative roughness pitch of 24, roughness angle of 90_ and 15,000 Reynolds number. This roughness arrangement gives friction factor of 0.031 with 3.48 Thermo hydraulic performance parameter. Statistical correlations were developed for Nusselt number, friction factor, Stanton number and thermo hydraulic performance parameter which give maximum average deviations below 12% with reasonable accuracy.

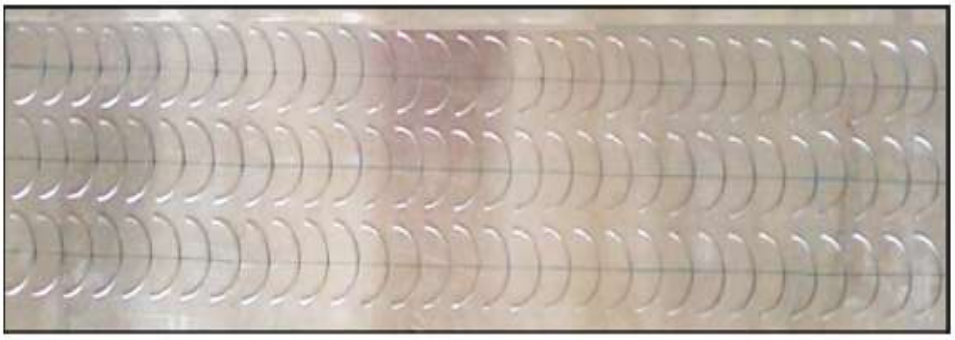

Figure 12 Multiple C-shape roughened absorber

2.8 Wedge shaped rib roughness

L.J.Bhagoria et al.,[37] studied heat transfer coefficient and friction factor correlation for rectangular solar air heater duct having transverse wedge shaped rib roughness on the absorber plate. They were used the range of parameters as shown in table no 3. Nusselt number increased up to 2.4 times while friction factor up to 5.3 times. The maximum heat transfer occurs for a relative roughness pitch of about 7.57, while the friction factor keeps decreasing as the relative roughness pitch increases. A maximum enhancement of heat transfer occurs at a wedge angle of about 10° while on either side of this wedge angle, Nusselt number decreases. The friction factor increases as the wedge angle increases.

Table 3. Range of parameters

Reynolds number, *Re*	3000–18000
Relative roughness height, e/D_h	0.015–0.033
Relative roughness pitch, p/e	$60.17\phi^{-1.0264} < p/e < 12.12$
Rib wedge angle, ϕ	8°–15°
Aspect ratio of duct, W/H	5

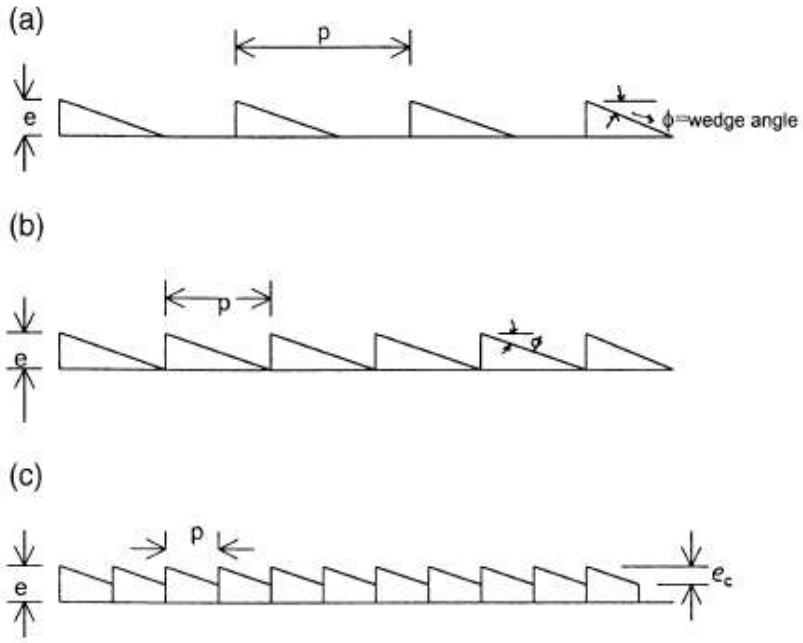

Figure 13 Wedge shaped rib geometries

2.9 Reverse L-shaped ribs roughness

Vipin B. Gawande et. al.,[38] experimentally and numerically studied reverse L-shaped rib (fig.14) roughness for forced convection heat transfer of air in a solar air heater. Thermal performance of solar air heater is studied with design variables such as relative roughness pitch ($7.14 \leq P/e \leq 17.86$), Reynolds number ($3800 \leq Re \leq 18{,}000$), heat flux (1000 W/m^2) and constant relative roughness height ($e/D = 0.042$). The maximum enhancement in Nusselt number has been found to be 2.827 times over the smooth duct corresponding to relative roughness pitch (P/e) of 7.14, relative roughness height (e/D) of 0.042 at Reynolds number (Re) of 15,000 in the range of parameters investigated and the maximum enhancement in the friction factor has been found to be 3.424 times over the smooth duct corresponding to relative roughness pitch (P/e) of 7.14, relative roughness height (e/D) of 0.042 at Reynolds number (Re) of 3800 in the range of parameters investigated. The optimum value of thermo–hydraulic performance parameter for reverse L-shaped rib configuration for the range of parameters investigated in the present system has been found to be 1.90 corresponding to relative roughness pitch (P/e) of 7.14, relative roughness height (e/D) of 0.042 and Reynolds number of 15,000. So, the present model can be employed for heat transfer augmentations.

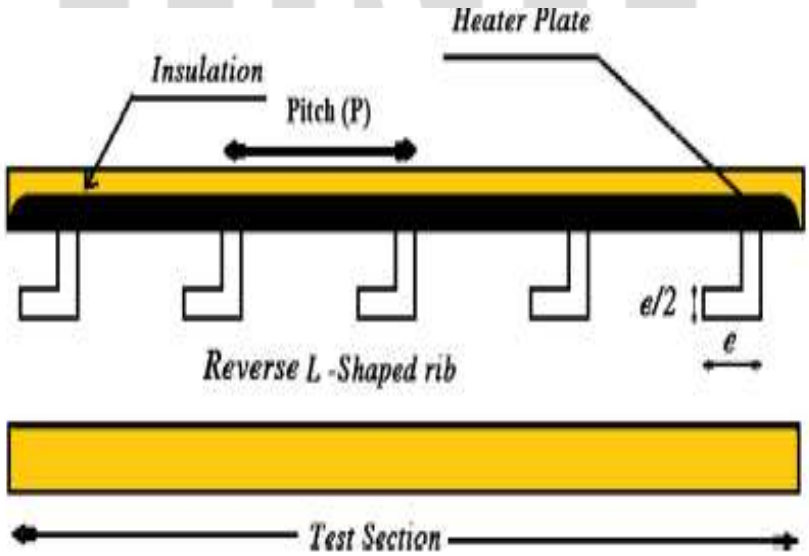

Figure 14 Reverse L-shaped rib roughness

2.10 W-shaped rib roughness

Atul Lanjewar et. al,.[39] carried out experimental investigation of heat transfer and friction factor characteristics of rectangular duct roughened with W-shaped ribs (fig.15). They have used duct with width to height ratio (W/H) of 8.0, relative roughness pitch (p/e) of 10, relative roughness height (e/D_h) 0.018-0.03375 and angle of attack of flow (a) 30-75°. Air flow rate corresponds to Reynolds number between 2300-14,000. They have noticed that rate of increase of Nusselt number with increasing Reynolds number is lower than rate of increase of friction factor because at higher values of relative roughness height, reattachment of free shear layer does not occur and rate of heat transfer enhancement is not proportional to that of friction factor. Maximum enhancement of Nusselt number and friction factor as result of providing artificial roughness has been found to be respectively 2.36 and 2.01 times that of smooth duct for angle of attack of 60°. Same angle of attack corresponds to maximum values of both Nusselt number and friction factor. Flow separation and secondary flow resulting from presence of W-shaped ribs and movement of vortices combine to give optimum value of angle of attack. Thermo-hydraulic performance improves with angle of attack of flow and relative roughness height and maxima occurs at angle of attack of 60°.

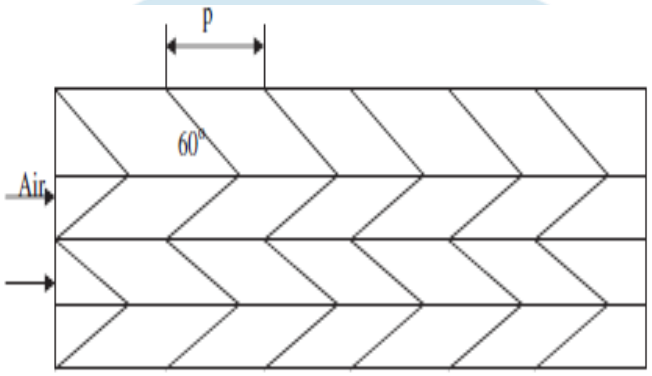

Figure 15 Schematic diagram of 60° W-shaped ribs

Arvind kumar et. al.,[40] experimentally investigated artificially roughened solar air heater duct with discrete W-shaped ribs as shown in fig.16. They were used aspect ratio as 8:1. Except the roughened wall all three walls were well insulated. The experiment encompassed Reynolds number (Re) range from 3000 to 15,000, relative roughness height (e/D_h) in the range of 0.0168–0.0338, relative roughness pitch (p/e) 10 and the angle of attack (α) in the range of 30–75°. Nusselt number increases with an increase of Reynolds number. The maximum enhancement of Nusselt number was found to be 1.44, 1.54, 1.67 and 1.61 times that for smooth duct for angles of attack of 30°, 45°, 60° and 75° for relative roughness height of 0.0168. Whereas for relative roughness height of 0.0338, the maximum enhancement in Nusselt number was found to be 1.88, 1.99, 2.16 and 2.08 times for corresponding angles of attack of 30°, 45°, 60° and 75°. Friction factor decreases with an increase of Reynolds number. For relative roughness height of 0.0168, the maximum enhancement in friction factor was found to be 1.53, 1.71, 1.82 and 1.76 times that of smooth duct for angles of attack of 30°, 45°, 60° and 75° respectively. Whereas for relative roughness height of 0.0338, the maximum enhancement was found to be 2.34, 2.61, 2.75 and 2.69 times for corresponding values of angles of attack of 30°, 45°, 60° and 75° respectively. The values of Nusselt number and friction factor are substantially higher as compared to those obtained for smooth absorber plates. This is due to distinct change in the friction characteristics as a result of roughness that causes flow separations, reattachments and the generation of secondary flows. The maximum enhancement of Nusselt number and friction factor as a result of providing artificial roughness has been found to be 2.16 and 2.75 times that of smooth duct for an angle of attack of 60°. It was observed that the same angle of attack corresponds to the maximum values of both Nusselt number and friction factor. It appears that the flow separation and the secondary flow resulting from the presence of discrete W-shaped ribs and the movement of resulting vortices combine to yield an optimum value of angle of attack.

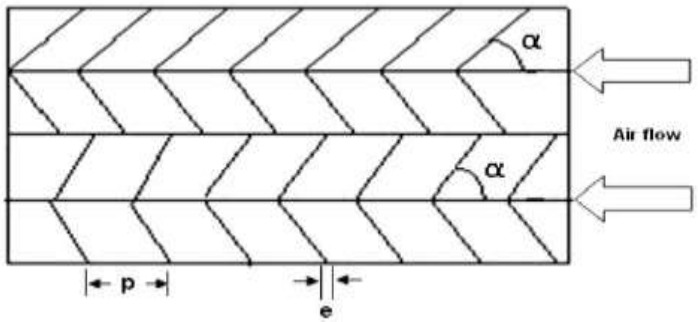

Figure 16 Discrete W-shaped ribs

2.11 Truncated rib roughness

Sanjay Sharma et. al.,[41] experimentally and numerically investigated the thin transverse and truncated ribs. They have used aspect ratio (W/H) of 10 for the duct, blockage ratio (e/H) is 0.1, relative roughness height (e/D_h) of 0.055, relative roughness pitch (P/e) of 10, angle of attack (α) of 90° and Reynolds number (Re) from 4000 to 16000. They considered four different rib arrangements to evaluate heat transfer, friction factor and thermo hydraulic performance parameter as shown in fig.17. The average Nusselt number (Nu_r) increases with Reynolds number for all the four different cases considered. The maximum average Nusselt number enhancement has been found to be 49.28 for case 1, for the range of parameters considered. The average friction factor increases with Reynolds number due to higher values of e/D_h (0.055) for all the cases. The maximum enhancement in normalized friction factor (f_r/f_0) is 2.88–7.18 for the case 4. The thermo hydraulic performance parameter (THPP) value is highest for the case 3. The average THPP value is 0.967 for the case 3 and the lowest is for case 2, which is 0.917. The experimental and three dimensional simulation results are in good agreement with the performed investigation.

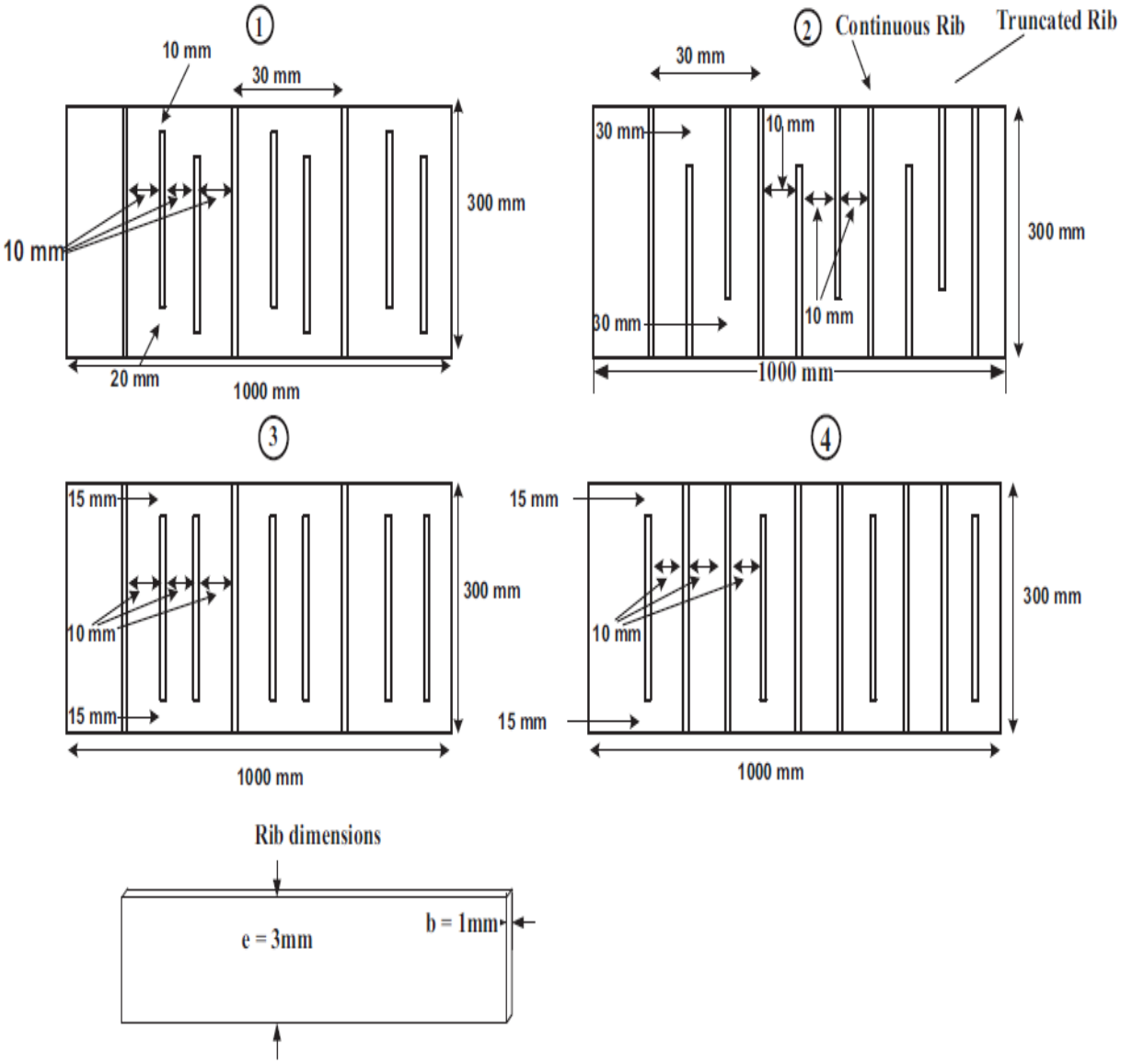

Figure 17 Different thin rib arrangements on absorber plate

2.12 Multiple arc with gap roughness

N.K.Pandey et. al.,[42] performed experiment for heat transfer augmentation using multiple arc gap as shown in fig.18. They used range of flow parameters as shown in table no.4. A good augmentation in Nu takes place by using multiple arcs with gap roughness configuration. Maximum augmentation achieved in Nu and f is 5.85 and 4.96 respectively. The maximum enhancement for Nu takes place at Reynolds number (Re) value of 21,000, g/e value of 1, d/x value of 0.65, W/w value of 5, e/D value of 0.044, p/e value of 8 and α/60 value of 1.

Table 4 Range of flow and roughness parameters

S. no.	Parameter	Range
1	Reynolds number (*Re*)	2100–21,000
2	Relative roughness pitch (*p*/*e*)	4–16
3	Relative roughness height (*e*/*D*)	0.016–0.044
4	Arc angle (α)	30–75°
5	Relative gap width (*g*/*e*)	0.5–2.0
6	Relative gap distance (*d*/*x*)	0.25–0.85
7	Aspect ratio (*W*/*H*)	10
8	Relative roughness width (*W*/*w*)	1–7

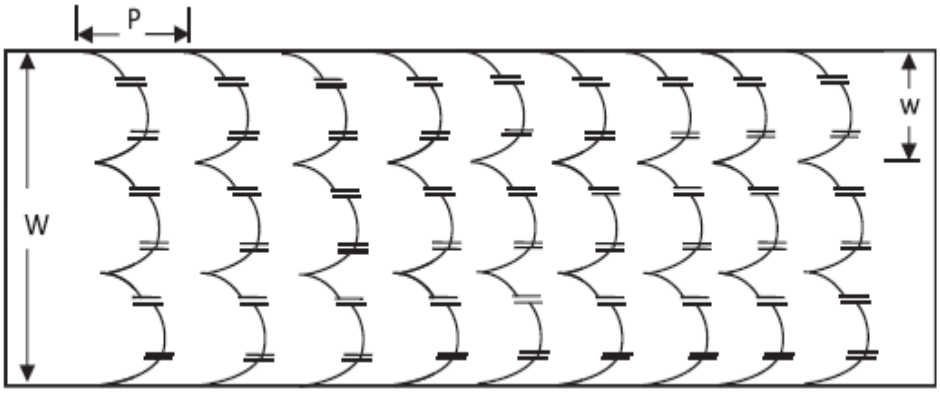

Figure 18 Multiple arc shaped ribs with gap[43]

2.13 Broken arc shaped roughness

V.S.Hans et. al.,[44] experimentally investigated solar air heater duct with aspect ratio 12 roughened with broken arc ribs (fig.19). Broken arcs were formed by symmetrical gap in continuous arcs. They used thirty seven broken arc rib with relative roughness pitch (P/e) 4-12, relative gap width (g/e) 0.5-2.5, relative gap position (d/w), relative roughness height (e/D_h) 0.022-0.043 and arc angle (α) 15°-75° and Reynolds number 2000-16000. For duct roughened with broken arc rib, the maximum enhancement in Nusselt number and friction factor over that of smooth duct have been found to be 2.63 and 2.44 times while the respective enhancements for continuous arc rib roughened duct have been found to be 1.19 and 1.14 times, for the parameters range investigated. These maximum enhancements corresponded to parameters combination of relative roughness pitch of 10, relative gap width of 1.0, arc angle of 30°, relative gap position of 0.65 and relative roughness height of 0.043.

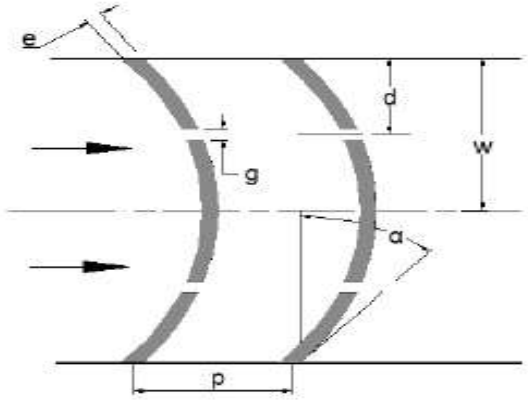

Figure 19 Broken arc ribs

R.S.Gill et. al.,[45] carried out experimental investigation of broken arc rib combined with staggered rib pieces (fig.20). The duct aspect ratio was 12 and absorber plat was heated with uniform heat flux except other three walls. The rib roughness has fixed

relative staggered rib position, relative roughness height, relative gap size, relative gap position, arc angle and relative roughness pitch of 0.4, 0.043, 1.0, 0.65, 30° and 10 respectively. The relative staggered rib size and Reynolds number were varied from 1 to 6 and 2000 to 16000 respectively. They have inferred that the staggered rib piece placed between two consecutive gaps of broken arc rib of roughened duct has strong influence on the friction factor and Nusselt number. Compared to smooth duct, the presence of staggered rib piece in broken arc rib enhanced the Nusselt number and friction factor by a factor up to 3.06 and 2.50 respectively, whereas in comparison to broken arc rib without staggered piece this enhancement was 2.60 and 2.27 respectively. The Nusselt number and friction factor values are maximum at relative staggered rib size of 4 and both decreased on either sides of this value.

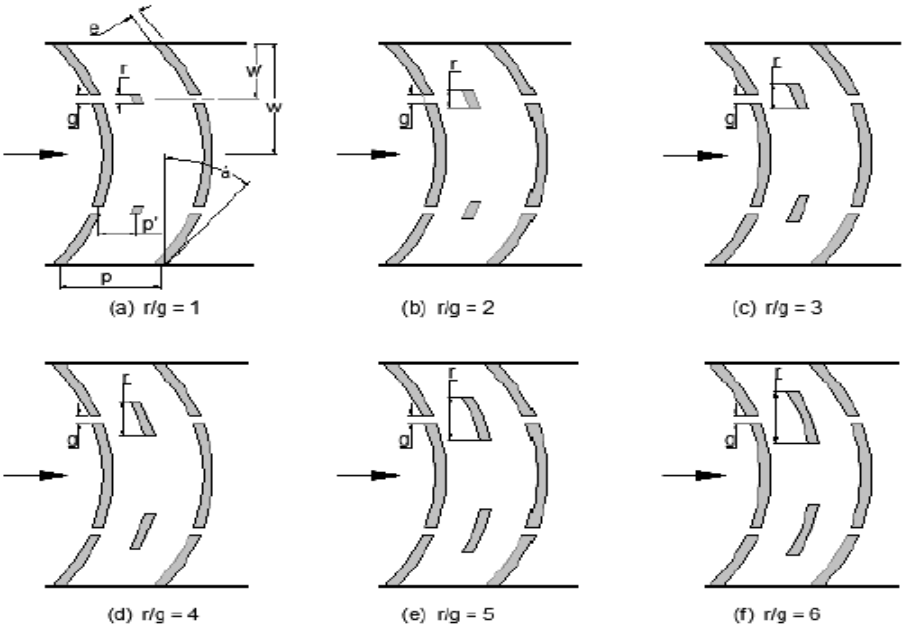

Figure 20 Broken arc rib combined with staggered rib

Table 5 Summary of the various roughness geometries used by various researchers

Authors	Roughness Geometry	Roughness	Results/Remarks
Dongxu Jin et al. [15]	Multi V-shaped ribs	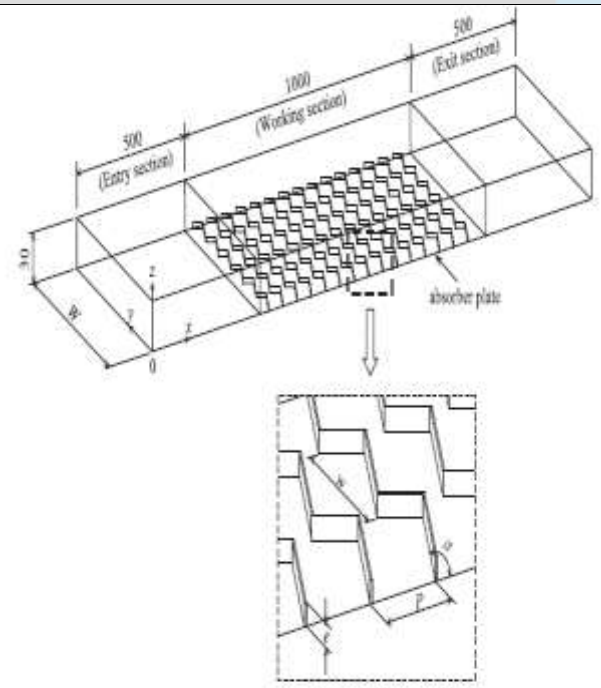	An angle of attack of 45° gives the maximum values of both the average Nusselt number and thermo hydraulic performance parameter, whereas an angle of attack of 60° gives the highest value of the friction factor.

Authors	Roughness Geometry	Roughness	Results/Remarks
P.K.Jain et al.[16]	New V-rib geometry	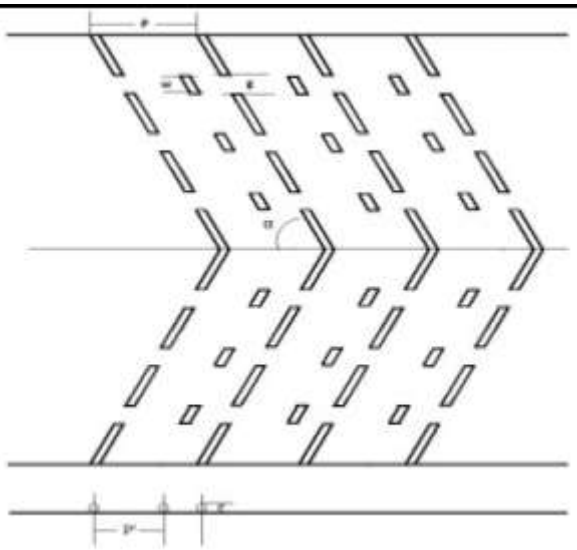	Multi gap V-down rib combined with staggered rib the enhancement in Nusselt number and friction factor is 2.27 and 3.35 times that of smooth plate respectively.
V.S.Hans et al.[18]	Multiple V-ribs	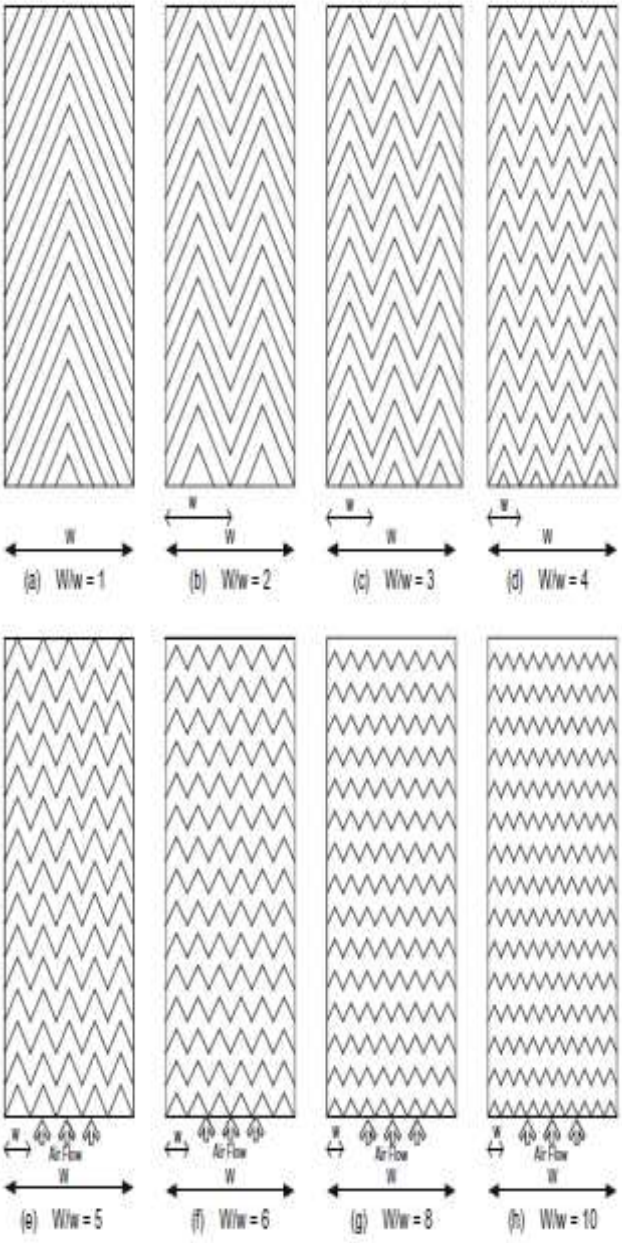	A maximum enhancement of Nusselt number and friction factor due to presence of such an artificial roughness has been found to be 6 and 5 times, respectively, in comparison to the smooth duct for the range of parameters considered.

Authors	Roughness Geometry	Roughness	Results/Remarks
P.Promvonge[19]	Multiple 60° V-baffles	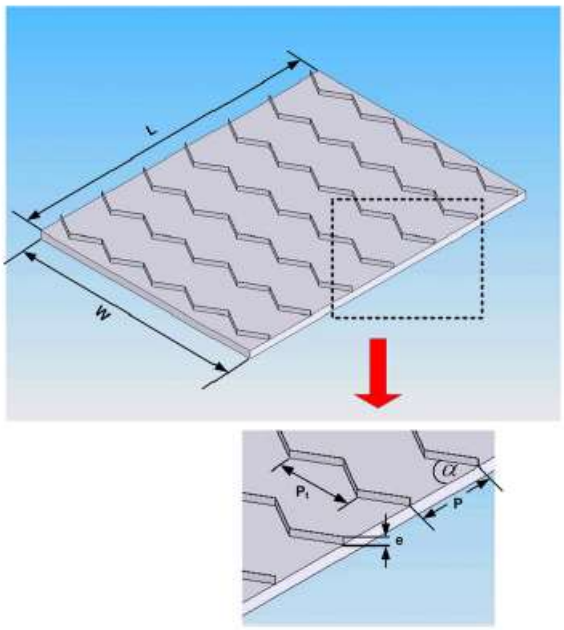	The Nusselt number augmentation tends to increase with the rise of Reynolds number. The use of the V-baffles with e/H=0.30 causes a very high heat transfer and pressure drop increase as compared with other flow blockage ratios.
S.Singh et al.[20]	V-down rib with gap	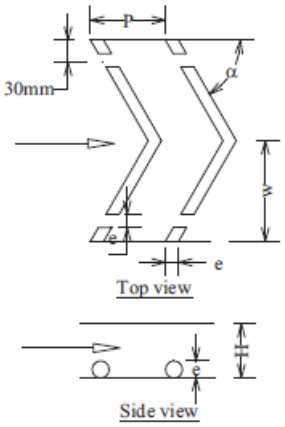	Both the Nusselt number and friction factor are strong function of relative roughness pitch. The highest value of Nusselt number and friction factor occurs at relative roughness pitch of 8 and both decrease on either side of this pitch value.
T.Alam et al.[23]	V-shaped perforated blocks	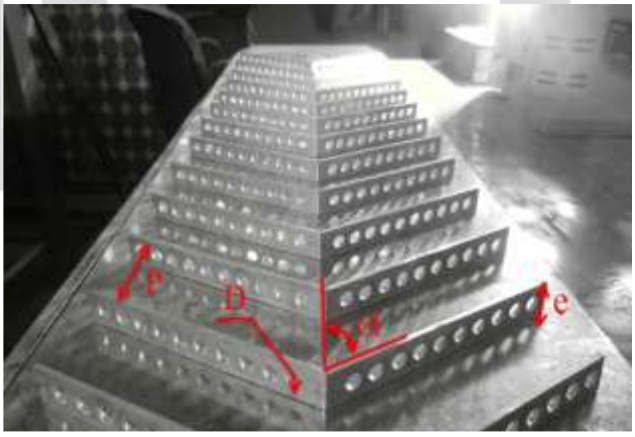	Providing the perforation in V-shaped blockages results in considerable enhancement in Nusselt number. Average enhancement in Nusselt number for perforated V-shaped blockages is found to be 33% higher over solid blockages while friction factor of perforated blockages gets decreased by 32% of the value as found in solid blockages.

Authors	Roughness Geometry	Roughness	Results/Remarks
R.Karwa et al.[24]	Half and fully perforated baffles	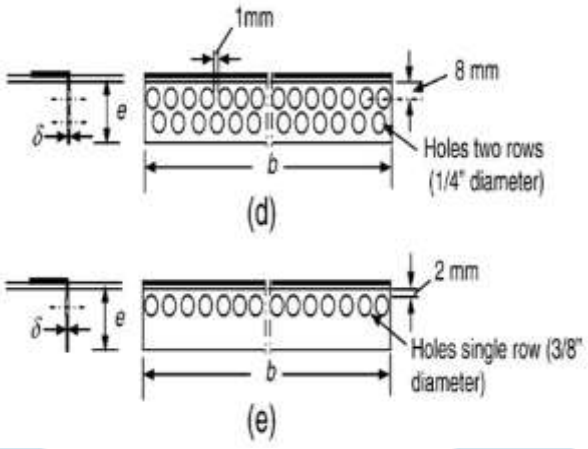 (d) fully perforated baffles (with two rows of holes), (e) half perforated baffles (with single row of holes)	An enhancement of 79–169% in Nusselt number over the smooth duct for the fully perforated baffles and 133–274% for the half perforated baffles while the friction factor for the fully perforated baffles is 2.98– 8.02 times of that for the smooth duct and is 4.42–17.5 times for the half perforated baffle
T.Alam et al.[25]	Circularity of perforation holes in V-shaped blocks	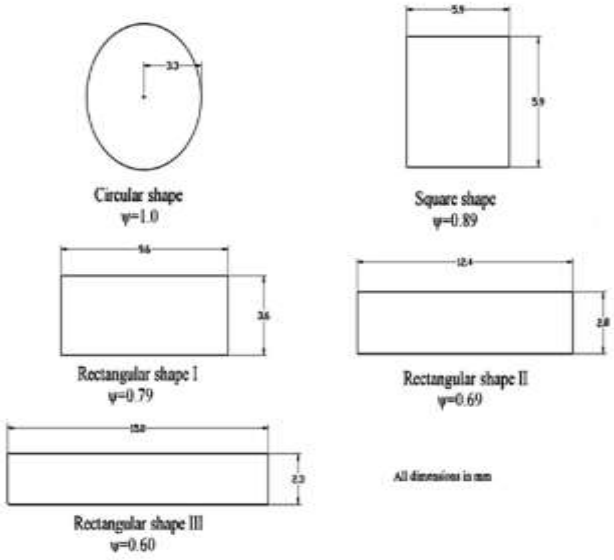 Five different shapes of perforation	Non-circular perforation holes was been found to result in higher heat transfer as compared to circular holes with same open area ratio; and there is optimum non-circular shape that corresponds to a circularity of 0.69.
S.Skullong et al.[26]	Perforated-winglet-type vortex generator	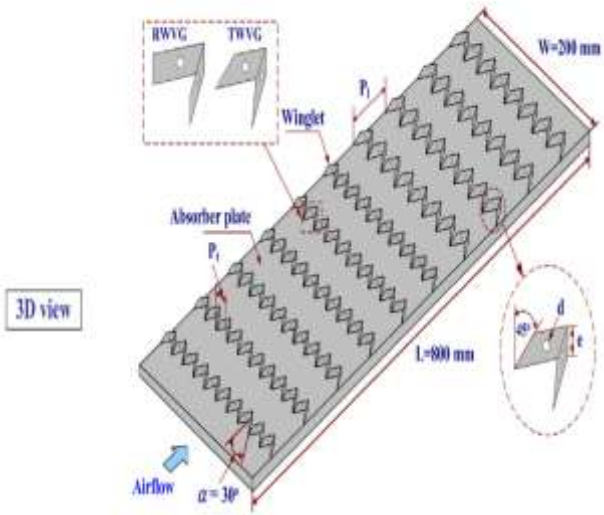	Heat transfer in SAH duct can be enhanced considerably by WVGs although friction loss is much high; the loss can be reduced by using P-WVGs.

Authors	Roughness Geometry	Roughness	Results/Remarks
P.Sriromreun et al.[30]	Z-shaped baffles	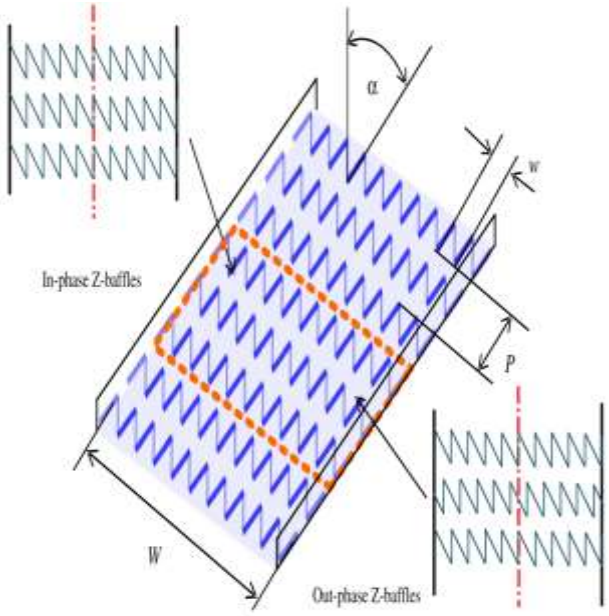	The in-phase Z- baffle performs better than the out-phase one. Also, the presence of the Z-baffle leads to a substantial increase in friction loss compared with the smooth channel with no baffle.
M.Sethi et al.[31]	Dimple shape roughness element		Nusselt number increases whereas friction factor decreases with the increase in Reynolds number. Values of friction factor and Nusselt number are higher as compared to the smooth ones.
Vikash Kumar[32]	Concave dimple shape roughness	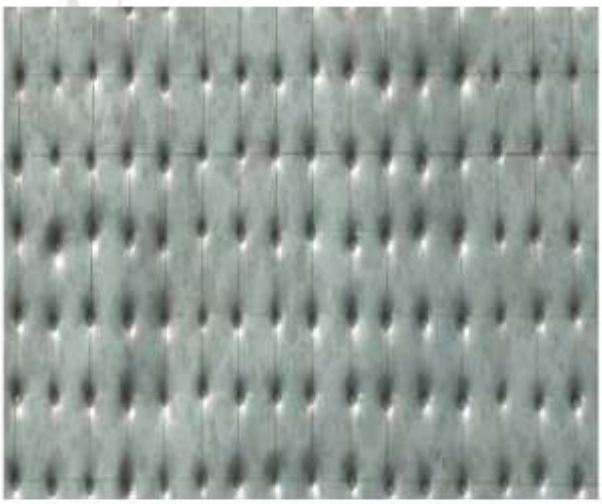	An increase in depth to diameter ratio resulted in an increase in Nusselt number from 1 to 1.5.

Authors	Roughness Geometry	Roughness	Results/Remarks
I.Singh et al.[33]	Multiple broken transverse ribs	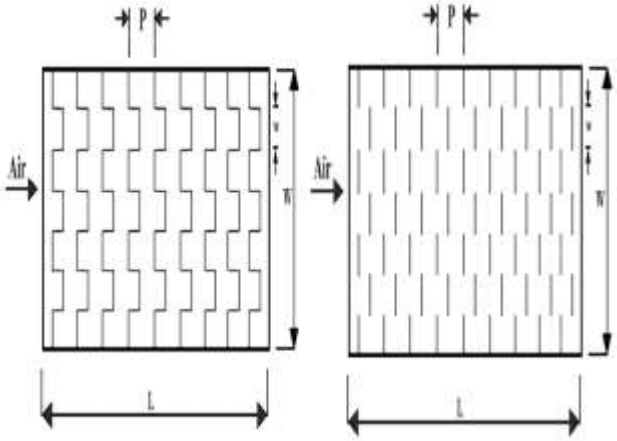 (a) Square wave shaped ribs (b) Multiple broken transverse ribs.	Nusselt number for multiple broken transverse ribs is more than square wave shaped ribs for the investigated Reynolds number range.
Varun et al.[34]	Transverse and inclined ribs	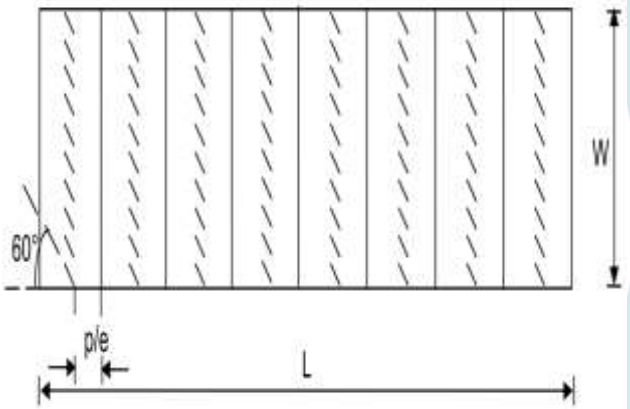	The maximum value of effective efficiency has been found for roughness parameters corresponding to relative roughness pitch (p/e) of 8 under the range of parameters investigated.
D.Wang et al.[35]	S-shaped ribs with gaps	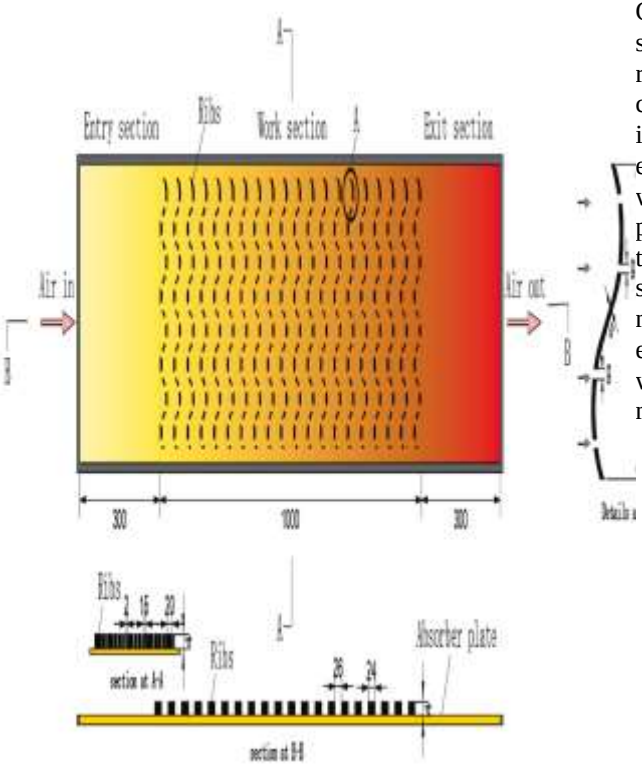	Compared to the smooth plate, the rough solar air heater can significantly increase the thermal efficiency of collector while increasing the pressure drop of air through the work section. The maximum thermal efficiency of collector was 65% at H=30 mm.

Authors	Roughness Geometry	Roughness	Results/Remarks
M.G. Gabhane et al.[36]	C-shape roughness	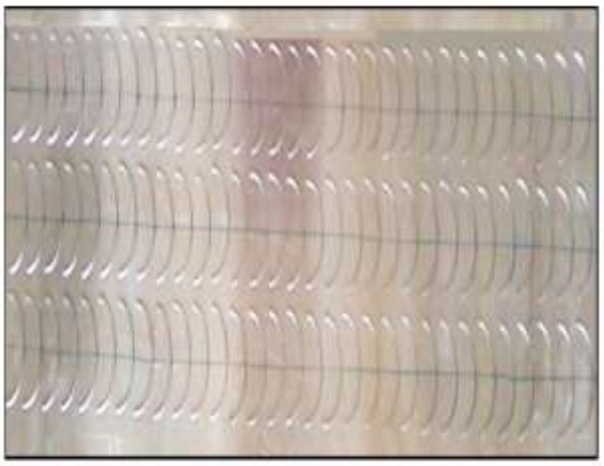	Multiple C-shape arrangement on both sides of absorber gives more heat transfer than scattered C-shape roughness.
J.L.Bhagoria[37]	Transverse wedge shape roughness	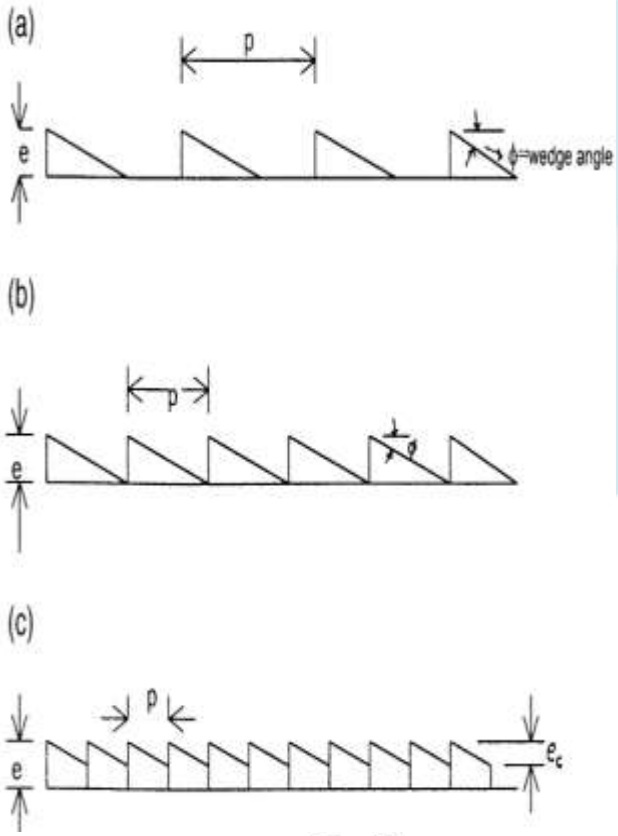	As compared to the smooth duct, the presence of ribs yields Nusselt number up to 2.4 times while the friction factor rises up to 5.3 times for the range of parameters investigated.
V.B.Gawande et al.[38]	Reverse L-shaped ribs	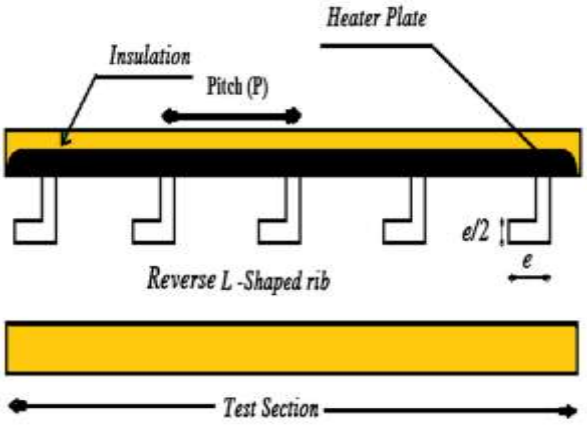	The maximum enhancement in Nusselt number has been found to be 2.827 times over the smooth duct corresponding to relative roughness pitch (P/e) of 7.14, relative roughness height (e/D) of 0.042 at Reynolds number (Re) of 15,000 in the range of parameters investigated.

Authors	Roughness Geometry	Roughness	Results/Remarks
A.Lanjewar et al.[39]	W-shape rib roughness	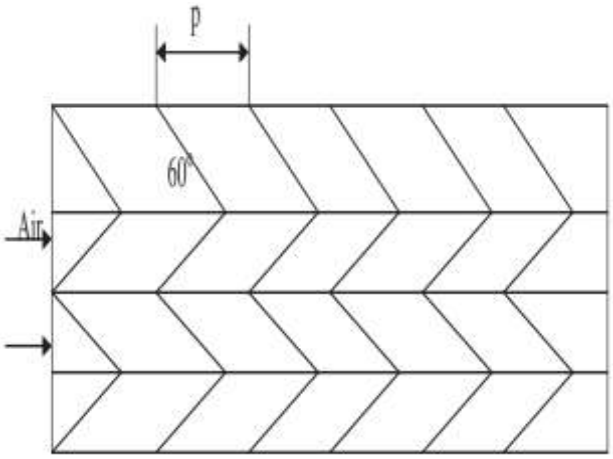	For relative roughness height of 0.03375 and at angle of attack of 60º W-shape ribs enhance value of Nusselt number by 2.21 times over smooth plate at Reynolds number of 14,000.
A.Kumar et al.[40]	Discrete W-shape ribs	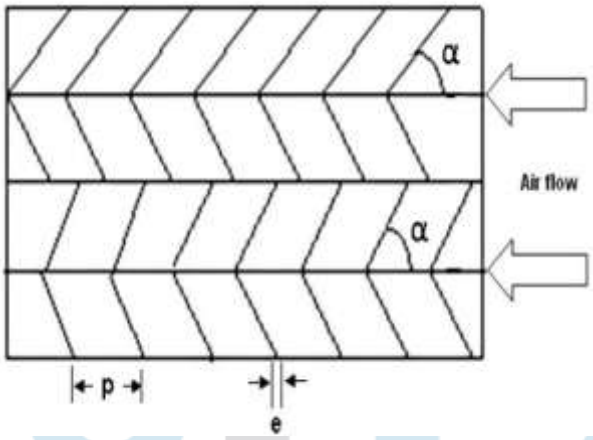	The maximum enhancement of Nusselt number and friction factor as a result of providing artificial roughness has been found to be 2.16 and 2.75 times that of smooth duct for an angle of attack of 60°.
S.K.Sharma et al.[41]	Thin transverse continuous and truncated ribs	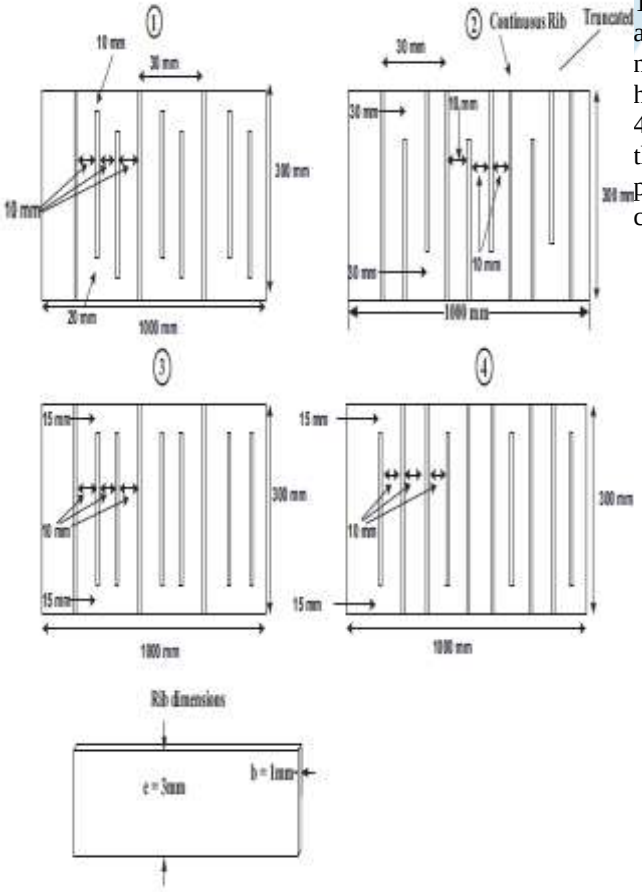	The maximum average Nusselt number enhancement has been found to be 49.28 for case 1, for the range of parameters considered.

Authors	Roughness Geometry	Roughness	Results/Remarks
N.K.Pandey et al.[42]	Multi arc with gap roughness	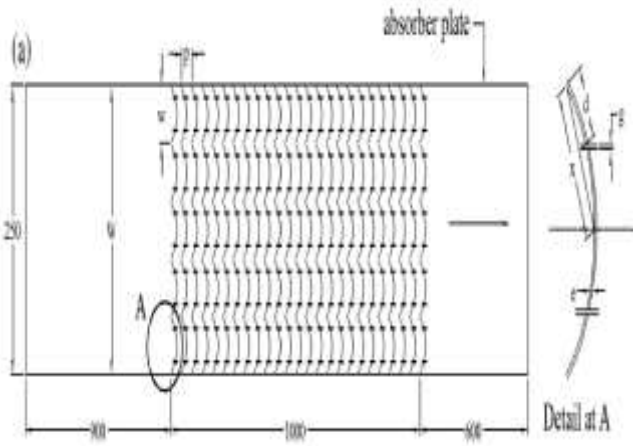	Maximum augmentation achieved in Nu and f is 5.85 and 4.96 respectively.
V.S.Hans et al. [44]	Broken arc ribs	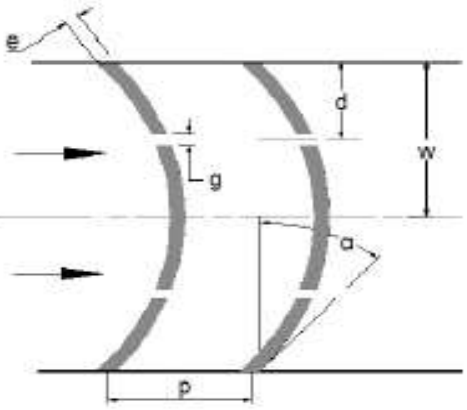	For duct roughened with broken arc rib, the maximum enhancement in Nusselt number and friction factor over that of smooth duct have been found to be 2.63 and 2.44 times respectively.
R.S.Gill et al.[45]	Staggered piece in a broken arc rib	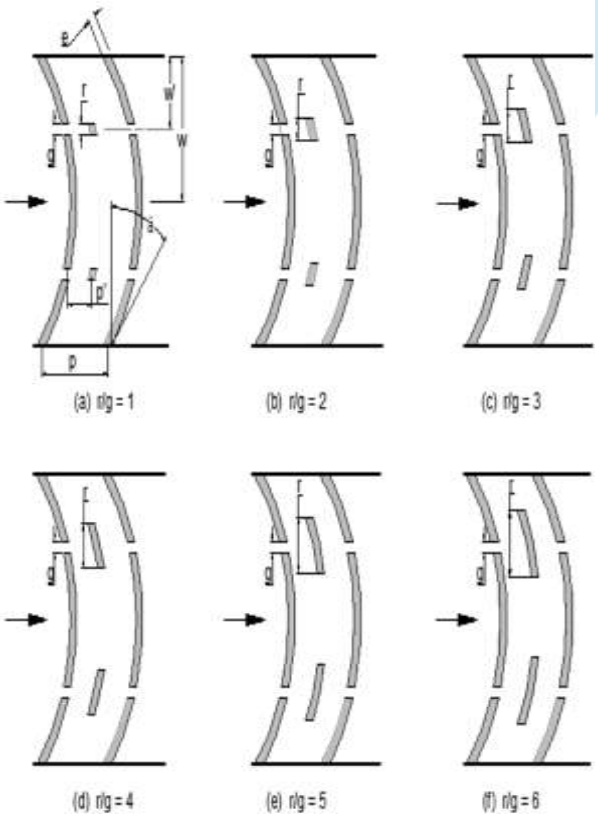	The Nusselt number and friction factor values are maximum at relative staggered rib size of 4 and both decreased on either sides of this value.

Conclusion

Solar air heater is widely used across the world for the industrial and domestic applications. The main problem for the solar air heater is its low thermal efficiency. Improving thermal efficiency is the main challenge for the researchers. Thermal efficiency can be improved by the heat transfer coefficient. Researchers have carried various experiments using various roughness geometries that help to improve the heat transfer coefficient. Artificial roughness generates the turbulence inside the fluid flow. Turbulence causes the higher heat transfer to the fluid. In this paper thorough review has been done for the different shapes of the roughness geometries. From the above comprehensive literature following conclusion can be made.

1. Use of the artificial roughness increases the heat transfer of the smooth absorber plate.
2. Artificial roughness increases the heat transfer at the same time it increases the pressure drop across the system.
3. Laminar sub-layer generated inside air duct during the fluid flow reduces the heat transfer between the absorber plate and the fluid, roughness geometries breaks the laminar sub-layer and increase the transfer.
4. Multi V-shaped ribs generate stream wise helical vortex flows, which promote the fluid mixing between the colder upper channel fluid and the warmer near-bottom-wall fluid. The V- shaped rib also induces a moving subsidiary vortex structure in the inter-rib region when a primary vortex flow moves across that region, and hence further enhances the local fluid mixing. Therefore, the heat transfer is greatly improved when compared to a smooth wall channel.
5. The staggered rib element placed directly in front of the gap in V-rib with symmetrical gap and staggered rib geometry has considerable effect on Nusselt number and friction factor.
6. Considerable heat transfer can be obtained by using multiple V ribs on absorber plate with uniform heat flux.
7. The use of the multiple 60º V-baffles with e/H=0.30 causes a very high heat transfer and pressure drop increase as compared with other flow blockage ratios. Multi V-shaped ribs generate stream wise helical vortex flows, which promote the fluid mixing between the colder upper- channel fluid and the warmer near-bottom-wall fluid. The V- shaped rib also induces a moving subsidiary vortex structure in the inter-rib region when a primary vortex flow moves across that region, and hence further enhances the local fluid mixing. Therefore, the heat transfer is greatly improved when compared to a smooth wall channel.
8. V-down rib with gap gives superior thermo hydraulic performance compare to multi V rib, discrete V shape rib, W- shape ribs.
9. Significant enhancement observed while providing perforation on V-shaped blocks. Half perforated baffles gives considerable augmentation than the fully perforated baffles at the same time friction factor values are higher for the half perforated baffles. Compare to the circular shapes non-circular shapes of perforation gives higher heat transfer.
10. Roughness geometry parameters such as relative pitch, relative roughness height, relative roughness depth, roughness gap, discretized distance etc. has great influence on the heat transfer and friction factor of the system.
11. Nusselt number is higher for the multiple broken transverse ribs compare to the square wave shaped ribs. The friction factor for multiple broken transverse ribs is lower than the square wave rib.
12. Multiple C-shape arrangement on both sides of absorber gives more heat transfer than scattered C-shape roughness while wedge shaped ribs causes low penalty of the frictional losses.
13. Discretized roughness elements are more efficient than the roughness geometries without discretization.
14. The staggered rib piece placed between two consecutive gaps of broken arc rib of roughened duct has strong influence on the friction factor and Nusselt number. Compared to smooth duct, the presence of staggered rib piece in broken arc rib enhanced the Nusselt number and friction factor by a factor up to 3.06 and 2.50 respectively, whereas in comparison to broken arc rib without staggered piece this enhancement was 2.60 and 2.27 respectively.

The review carried out in this paper intended to help researchers to design and modify the SAH and give an overview of various methods to increase the thermal performance of the solar air heater. Developments with this regards promotes the conservation of energy and sustainable energy developments.

Future scope

1. There is more research is required in context with material and configuration of the system for solar air heater that can cause cost reduction and make system more compact.
2. More future research can be done for the various roughness geometries like V-shape, W shape, reverse L shape and S-shape roughness to obtain set of the optimum roughness parameters for the various roughness geometries.
3. Combination of the different roughness geometries can also be used to get their combined influence to increase the thermal performance of the SAH system.

References

[1] A. Singh Yadav and M. Kumar Thapak, "Artificially roughened solar air heater: Experimental investigations," *Renew. Sustain. Energy Rev.*, vol. 36, pp. 370–411, 2014, doi: 10.1016/j.rser.2014.04.077.

[2] H. Gupta and S. K. Gupta, "Conventional and Non-Conventional Energy Resources of India : Present and Future," *Etme*, no. February, pp. 70–76, 2011.

[3] P. K. Gupta, "Renewable energy sources-a longway to go in India," *Renew. Energy*, vol. 16, no. 1-4–4 pt 2, pp. 1216–1219, 1999, doi: 10.1016/S0960-1481(98)00486-8.

[4] "' Experimental Analysis on Heat Transfer Enhancement in a Solar Air Channel Using Combined Modified Z-Shape and Dimpled Baffles ,'" 2019.

[5] L. Evangelisti, R. De Lieto Vollaro, and F. Asdrubali, "Latest advances on solar thermal collectors: A comprehensive review," *Renew. Sustain. Energy Rev.*, vol. 114, no. March, 2019, doi: 10.1016/j.rser.2019.109318.

[6] V. V. Tyagi, N. L. Panwar, N. A. Rahim, and R. Kothari, "Review on solar air heating system with and without thermal energy storage system," *Renew. Sustain. Energy Rev.*, vol. 16, no. 4, pp. 2289–2303, 2012, doi: 10.1016/j.rser.2011.12.005.

[7] H. S. Arunkumar, K. Vasudeva Karanth, and S. Kumar, "Review on the design modifications of a solar air heater for improvement in the thermal performance," *Sustain. Energy Technol. Assessments*, vol. 39, no. January, p. 100685, 2020, doi: 10.1016/j.seta.2020.100685.

[8] N. K. Bansal, "Solar air heater applications in India," *Renew. Energy*, vol. 16, no. 1-4–4 pt 2, pp. 618–623, 1999, doi: 10.1016/S0960-1481(98)00237-7.

[9] S. R. H. Mohideen, "Solar Air Heater," *Aust. Plan.*, vol. 21, no. 1, p. 24, 1983, doi: 10.1080/07293682.1983.9657057.

[10] X. Li, G. Yuan, Z. Wang, H. Li, and Z. Xu, "Experimental study on a humidification and dehumidification desalination system of solar air heater with evacuated tubes," *Desalination*, vol. 351, pp. 1–8, 2014, doi: 10.1016/j.desal.2014.07.008.

[11] H. Henning, "Solar air-conditioning and refrigeration - achievements and challenges," 2010.

[12] A. Kumar *et al.*, "Developing heat transfer and pressure loss in an air passage with multi discrete V-blockages," *Exp. Therm. Fluid Sci.*, vol. 84, pp. 266–278, 2017, doi: 10.1016/j.expthermflusci.2017.02.017.

[13] J. Hu and G. Zhang, "Performance improvement of solar air collector based on airflow reorganization: A review," *Appl. Therm. Eng.*, vol. 155, pp. 592–611, 2019, doi: 10.1016/j.applthermaleng.2019.04.021.

[14] M. M. Sahu and J. L. Bhagoria, "Augmentation of heat transfer coefficient by using 90° broken transverse ribs on absorber plate of solar air heater," *Renew. Energy*, vol. 30, no. 13, pp. 2057–2073, 2005, doi: 10.1016/j.renene.2004.10.016.

[15] D. Jin, M. Zhang, P. Wang, and S. Xu, "Numerical investigation of heat transfer and fluid flow in a solar air heater duct with multi V-shaped ribs on the absorber plate," *Energy*, vol. 89, pp. 178–190, 2015, doi: 10.1016/j.energy.2015.07.069.

[16] P. K. Jain and A. Lanjewar, "Overview of V-RIB geometries in solar air heater and performance evaluation of a new V-RIB geometry," *Renew. Energy*, vol. 133, pp. 77–90, 2019, doi: 10.1016/j.renene.2018.10.001.

[17] P. Pitak, E. A. Petpices, J. Withada, and E. A. Smith, "Turbulent heat transfer and pressure loss in a square channel with discrete broken V-rib turbulators," *J. Hydrodyn.*, vol. 28, no. 2, pp. 275–283, 2016, doi: 10.1016/S1001-6058(16)60629-7.

[18] V. S. Hans, R. P. Saini, and J. S. Saini, "Heat transfer and friction factor correlations for a solar air heater duct roughened artificially with multiple v-ribs," *Sol. Energy*, vol. 84, no. 6, pp. 898–911, 2010, doi: 10.1016/j.solener.2010.02.004.

[19] P. Promvonge, "Heat transfer and pressure drop in a channel with multiple 60° V-baffles," *Int. Commun. Heat Mass Transf.*, vol. 37, no. 7, pp. 835–840, 2010, doi: 10.1016/j.icheatmasstransfer.2010.04.003.

[20] S. Singh, S. Chander, and J. S. Saini, "Thermo-hydraulic performance due to relative roughness pitch in V-down rib with gap in solar air heater duct - Comparison with similar rib roughness geometries," *Renew. Sustain. Energy Rev.*, vol. 43, pp. 1159–1166, 2015, doi: 10.1016/j.rser.2014.11.087.

[21] A. M. Ebrahim Momin, J. S. Saini, and S. C. Solanki, "Heat transfer and friction in solar air heater duct with V-shaped rib roughness on absorber plate," *Int. J. Heat Mass Transf.*, vol. 45, no. 16, pp. 3383–3396, 2002, doi: 10.1016/S0017-9310(02)00046-7.

[22] N. S. Deo, S. Chander, and J. S. Saini, "Performance analysis of solar air heater duct roughened with multigap V-down ribs combined with staggered ribs," *Renew. Energy*, vol. 91, pp. 484–500, 2016, doi: 10.1016/j.renene.2016.01.067.

[23] T. Alam, R. P. Saini, and J. S. Saini, "Experimental investigation on heat transfer enhancement due to V-shaped perforated blocks in a rectangular duct of solar air heater," *Energy Convers. Manag.*, vol. 81, pp. 374–383, 2014, doi: 10.1016/j.enconman.2014.02.044.

[24] R. Karwa and B. K. Maheshwari, "Heat transfer and friction in an asymmetrically heated rectangular duct with half and fully perforated baf fl es at different pitches ☆," *Int. Commun. Heat Mass Transf.*, vol. 36, no. 3, pp. 264–268, 2009, doi: 10.1016/j.icheatmasstransfer.2008.11.005.

[25] T. Alam, R. P. Saini, and J. S. Saini, "Effect of circularity of perforation holes in V-shaped blockages on heat transfer and friction characteristics of rectangular solar air heater duct," *Energy Convers. Manag.*, vol. 86, pp. 952–963, 2014, doi: 10.1016/j.enconman.2014.06.050.

[26] S. Skullong, P. Promthaisong, P. Promvonge, C. Thianpong, and M. Pimsarn, "Thermal performance in solar air heater with perforated-winglet-type vortex generator," *Sol. Energy*, vol. 170, no. August 2017, pp. 1101–1117, 2018, doi: 10.1016/j.solener.2018.05.093.

[27] J. J. Hwang and T. M. Liou, "Heat transfer in a rectangular channel with perforated turbulence promoters using holographic interferometry measurement," *Int. J. Heat Mass Transf.*, vol. 38, no. 17, pp. 3197–3207, 1995, doi: 10.1016/0017-9310(95)00065-H.

[28] O. N. Sara, T. Pekdemir, S. Yapici, and M. Yilmaz, "Heat-transfer enhancement in a channel flow with perforated rectangular blocks," *Int. J. Heat Fluid Flow*, vol. 22, no. 5, pp. 509–518, 2001, doi: 10.1016/S0142-727X(01)00117-5.

[29] T. M. Liou and S. H. Chen, "Turbulent heat and fluid flow in a passage disturbed by detached perforated ribs of different heights," *Int. J. Heat Mass Transf.*, vol. 41, no. 12, pp. 1795–1806, 1998, doi: 10.1016/S0017-9310(97)00242-1.

[30] P. Sriromreun, C. Thianpong, and P. Promvonge, "Experimental and numerical study on heat transfer enhancement in a channel with Z-shaped baffles," *Int. Commun. Heat Mass Transf.*, vol. 39, no. 7, pp. 945–952, 2012, doi: 10.1016/j.icheatmasstransfer.2012.05.016.

[31] M. Sethi and N. S. Thakur, "Correlations for solar air heater duct with dimpled shape roughness elements on absorber plate," *Sol. Energy*, vol. 86, no. 9, pp. 2852–2861, 2012, doi: 10.1016/j.solener.2012.06.024.

[32] V. Kumar, "Nusselt number and friction factor correlations of three sides concave dimple roughened solar air heater," *Renew. Energy*, vol. 135, pp. 355–377, 2019, doi: 10.1016/j.renene.2018.12.002.

[33] I. Singh, S. Vardhan, S. Singh, and A. Singh, "Experimental and CFD analysis of solar air heater duct roughened with multiple broken transverse ribs: A comparative study," *Sol. Energy*, vol. 188, no. February, pp. 519–532, 2019, doi: 10.1016/j.solener.2019.06.022.

[34] Varun, A. Patnaik, R. P. Saini, S. K. Singal, and Siddhartha, "Performance prediction of solar air heater having roughened duct provided with transverse and inclined ribs as artificial roughness," *Renew. Energy*, vol. 34, no. 12, pp. 2914–2922, 2009, doi: 10.1016/j.renene.2009.04.030.

[35] D. Wang, J. Liu, Y. Liu, Y. Wang, B. Li, and J. Liu, "Evaluation of the performance of an improved solar air heater with 'S' shaped ribs with gap," *Sol. Energy*, vol. 195, no. 13, pp. 89–101, 2020, doi: 10.1016/j.solener.2019.11.034.

[36] M. G. Gabhane and A. B. Kanase-Patil, "Experimental analysis of double flow solar air heater with multiple C shape roughness," *Sol. Energy*, vol. 155, pp. 1411–1416, 2017, doi: 10.1016/j.solener.2017.07.038.

[37] J. L. Bhagoria, J. S. Saini, and S. C. Solanki, "Heat transfer coefficient and friction factor correlations for rectangular solar air heater duct having transverse wedge shaped rib roughness on the absorber plate," *Renew. Energy*, vol. 25, no. 3, pp. 341–369, 2002, doi: 10.1016/S0960-1481(01)00057-X.

[38] V. B. Gawande, A. S. Dhoble, D. B. Zodpe, and S. Chamoli, "ScienceDirect Experimental and CFD investigation of convection heat transfer in solar air heater with reverse L-shaped ribs," *Sol. ENERGY*, vol. 131, pp. 275–295, 2016, doi: 10.1016/j.solener.2016.02.040.

[39] A. Lanjewar, J. L. Bhagoria, and R. M. Sarviya, "Heat transfer and friction in solar air heater duct with W-shaped rib roughness on absorber plate," *Energy*, vol. 36, no. 7, pp. 4531–4541, 2011, doi: 10.1016/j.energy.2011.03.054.

[40] A. Kumar, J. L. Bhagoria, and R. M. Sarviya, "Heat transfer and friction correlations for artificially roughened solar air heater duct with discrete W-shaped ribs," *Energy Convers. Manag.*, vol. 50, no. 8, pp. 2106–2117, 2009, doi: 10.1016/j.enconman.2009.01.025.

[41] S. K. Sharma and V. R. Kalamkar, "Experimental and numerical investigation of forced convective heat transfer in solar air heater with thin ribs," *Sol. Energy*, vol. 147, pp. 277–291, 2017, doi: 10.1016/j.solener.2017.03.042.

[42] N. K. Pandey, V. K. Bajpai, and Varun, "Experimental investigation of heat transfer augmentation using multiple arcs with gap on absorber plate of solar air heater," *Sol. Energy*, vol. 134, pp. 314–326, 2016, doi: 10.1016/j.solener.2016.05.007.

[43] V. S. Bisht, A. K. Patil, and A. Gupta, "Review and performance evaluation of roughened solar air heaters," vol. 81, no. July 2017, pp. 954–977, 2018.

[44] V. S. Hans, R. S. Gill, and S. Singh, "Heat transfer and friction factor correlations for a solar air heater duct roughened artificially with broken arc ribs," *Exp. Therm. Fluid Sci.*, vol. 80, pp. 77–89, 2017, doi: 10.1016/j.expthermflusci.2016.07.022.

[45] R. S. Gill, V. S. Hans, J. S. Saini, and S. Singh, "Investigation on performance enhancement due to staggered piece in a broken arc rib roughened solar air heater duct," *Renew. Energy*, vol. 104, pp. 148–162, 2017, doi: 10.1016/j.renene.2016.12.002.